Ecological Informatics 69 (2022) 101601

Contents lists available at ScienceDirect

Ecological Informatics

journal homepage: www.elsevier.com/locate/ecolinf

PermaBN: A Bayesian Network framework to help predict permafrost thaw in the Arctic

Katherine Beall [a], Julie Loisel [a,*], Zenon Medina-Cetina [b,*]

[a] Texas A&M University, Department of Geography, USA
[b] Texas A&M University, Zachry Department of Civil and Environmental Engineering, USA

ARTICLE INFO

Keywords:
Bayesian modeling
Probabilistic modeling
Environmental modeling
Ecological modeling
Uncertainty
Expert assessment

ABSTRACT

Rising global temperatures are a threat to the current state of the Arctic. In particular, permafrost degradation has been impacting the terrestrial cryosphere in many ways, including effects on carbon cycling and the global climate, regional hydrological connectivity and ecosystem dynamics, as well as human health and infrastructure. However, the ability to simulate permafrost dynamics under future climate projections is limited, and model outputs are often associated with large uncertainties. A model structured on a Bayesian Network is presented to address existing limitations in the representation of physically complex processes and the limited availability of observational data. A strength of Bayesian methods over more traditional modeling methods is the ability to integrate various types of evidence (i.e., observations, model outputs, expert assessments) into a single model by mapping the evidence into probability distributions. Here, we outline PermaBN, a new modeling framework, to simulate permafrost thaw in the continuous permafrost region of the Arctic. Pre-validation and expert assessment validation results show that the model produces estimations of permafrost thaw depth that are consistent with current research, i.e., thaw depth increases during the snow-free season under initial conditions favoring warming temperatures, lowered soil moisture conditions, and low active layer ice content. Using a case study from northwestern Canada to evaluate PermaBN, we show that model performance is enhanced when certainty about the system components increases for known scenarios described by observations directly integrated into the model; in this case, insulation properties from vegetation were integrated to the model. Overall, PermaBN could provide informative predictions about permafrost dynamics without high computational cost and with the ability to integrate multiple types of evidence that traditional physics-based models sometimes do not account for, allowing PermaBN to be applied to carbon modeling studies, infrastructure hazard assessments, and policy decisions aimed at mitigation of, and adaptation to, permafrost degradation.

1. Introduction

In the face of warming global temperatures, the Arctic is undergoing rapid change (IPCC, 2013; Schuur and Mack, 2018; Serreze and Barry, 2014). The cryosphere, which encapsulates all portions of Earth's surface that are covered in frozen water, is particularly vulnerable to current and future warming. Decreasing trends and record lows in sea ice extents and thicknesses have been observed in recent decades, in addition to prolonged summer melt seasons and ice sheet loss (Comiso et al., 2008; Hanna et al., 2020; Kwok et al., 2009; Serreze et al., 2007; Serreze and Meier, 2019; Stroeve et al., 2014). In marine ecosystems, the consequences of sea ice loss include increased sea surface temperatures (Stroeve et al., 2014), habitat loss for marine mammals (Laidre et al., 2008), and the amplification of Arctic temperatures (Pistone et al., 2014; Screen and Simmonds, 2010; Serreze et al., 2009). On land, permafrost is increasingly vulnerable to degradation (Biskaborn et al., 2019; Jorgenson et al., 2010; Koven et al., 2013; Turetsky et al., 2020). Permafrost thaw has direct consequences for both the natural environment and human communities (Schuur and Mack, 2018), including damage to built infrastructure (Hjort et al., 2018; Karjalainen et al., 2019), landscape change through the creation of thermokarst terrain (Kokelj and Jorgenson, 2013; Olefeldt et al., 2016), and release of previously frozen soil carbon (Schuur et al., 2009; Schuur et al., 2015).

In recent decades, the temperatures of circumpolar permafrost have increased by 2–4 °C (Kokelj and Jorgenson, 2013) as a result of Earth's northernmost latitudes warming at a rate twice as fast as the global

* Corresponding authors at: 3147 TAMU, College Station, TX 77843, USA.
E-mail addresses: julieloisel@tamu.edu (J. Loisel), zenon@tamu.edu (Z. Medina-Cetina).

https://doi.org/10.1016/j.ecoinf.2022.101601
Received 1 December 2021; Received in revised form 12 February 2022; Accepted 12 February 2022
Available online 17 February 2022
1574-9541/© 2022 The Authors. Published by Elsevier B.V. This is an open access article under the CC BY-NC-ND license (http://creativecommons.org/licenses/by-nc-nd/4.0/).

average (IPCC, 2013). Warming temperatures are often associated with permafrost thaw and degradation, but permafrost is not directly connected to the atmosphere. Instead, the ground thermal regime, along with soil properties, snow, surface and subsurface hydrology, vegetation, and topography, mediate permafrost stability (Gockede et al., 2019; Jorgenson et al., 2010; Stiegler et al., 2016; Zhang et al., 2018). Likewise, just as these factors control permafrost stability, permafrost also controls these properties and processes. For instance, permafrost acts as a structural component for regulating ecosystems through its impact on temperature, water, and nutrients. Active layer depth controls the temperature regime of soil layers, with soil near the bottom of the active layer remaining only a degree or two above freezing when thawed; temperature also affects SOM decomposition and plant and animal physiology (Schuur and Mack, 2018). The presence of permafrost, especially ice-rich permafrost, affects water flow paths and water availability by decreasing infiltration and increasing evaporation and runoff when water sits on the surface of the upper thaw layer; this has implications for plant access to water and whether heterotrophic organisms are exposed to aerobic or anaerobic conditions (Schuur and Mack, 2018). Permafrost also controls nutrient availability, primarily of nitrogen, through seasonal thaw depth and permafrost temperature; near-freezing temperatures inhibit nitrogen release by microorganisms (Schuur and Mack, 2018).

The extent of permafrost also alters surface topography and the distribution of vegetation communities across landscapes. For example, in the tundra, water infiltration is limited due to the frozen ground; as such, vegetation is primarily limited to nonvascular mosses and lichens that lack root systems (Schuur and Mack, 2018). In the boreal region, conditions are more favorable for water infiltration, contributing to taller vegetation coverage (along with warmer growing seasons); ground subsidence due to thawing of ice-rich ground is also less common than in the tundra (Jorgenson and Osterkamp, 2005). Along those lines, factors that control permafrost thaw may differ between these two regions. For instance, taller vegetation can contribute to higher snow depths, thereby altering the ground thermal regime and accelerating permafrost degradation; increased surface water coverage can also accelerate permafrost degradation through surface energy fluxes (Burn and Kokelj, 2009).

To gain a better understanding of how the Arctic will change in a warming world and assess the consequences of permafrost degradation, many researchers and stakeholders rely on models to inform their studies or decisions (Flynn et al., 2019; Koven et al., 2013). While there is a general understanding of how permafrost thaw is impacted by various feedbacks and surface properties (Gockede et al., 2019; Jorgenson et al., 2010; Schuur and Mack, 2018; Stiegler et al., 2016; Zhang et al., 2018), current research emphasizes the need to further improve permafrost modeling and address model shortcomings (Lawrence et al., 2008; Riseborough, 2007; Tao et al., 2017). Often-cited deficiencies include difficulties with (or lack of) the representation of the ground thermal regime and vegetation dynamics, limitations inherent to the modeling approach adopted (e.g., fixed temporal domain in equilibrium models or requirement of spatial data for numerical models), and heterogeneity in variable conditions (Lawrence et al., 2008; Riseborough, 2007; Tao et al., 2017). Many studies aim at addressing these known issues and improving existing models or modeling approaches (e.g., Jafarov et al. (2012), Tao et al. (2017), Westermann et al. (2016)). While these advancements are essential, alternative modeling methods that allow for the integration of different data types should be further explored.

To address the difficulty in simulating permafrost thaw under future projected climate conditions with current models, this paper presents a new modeling framework (PermaBN) in the form of a Bayesian Network (BN). This approach allows explicit representation of the variables related to permafrost thaw and simulation of changes in permafrost thaw depth by identifying critical variables and processes contributing to permafrost thaw, by defining their cause-effect relations, and by estimating the state of these variables and processes using probability density functions. The potential to integrate available observational data, model predictions, and expert assessments to represent the state of each participating variable and process in the PermaBN model using probability densities (Medina-Cetina and Nadim, 2008) allows us to link the main geological and atmospheric components of the Arctic system that influence permafrost thaw depth, along with surface insulation properties and key soil characteristics. The BN performance is then evaluated relative to an existing case study from northwestern Canada (Wilcox et al., 2019).

2. Background

2.1. Existing permafrost models

There is a substantial research interest in gaining a greater understanding of how the Arctic will change in a warming world. As permafrost is a key component of the terrestrial Arctic system, there is a long history of observations, experiments, and models that have been made to better understand its spatial and temporal dynamics. While Arctic observational networks have improved over the years (e.g., Global Terrestrial Network for Permafrost), many regions remain under sampled and understudied (Biskaborn et al., 2015; Gruber, 2012; Serreze and Barry, 2014). Models are often relied on to fill these data and knowledge gaps by extrapolating known scenarios where system conditions are calibrated and tested, to other similar scenarios where data is not available.

The breadth and complexity of existing permafrost models varies. Some of the first permafrost models used empirical, analytical, and/or physically-based/equilibrium modeling approaches. Empirical models are developed using observations and focused on describing data, such as relationships that can be used for forecasting; they can be either deterministic or probabilistic (e.g., Keller (1992), Lunardini (1978), and Nelson and Outcalt (1987)). In contrast, analytical models are based on formulations (analytic functions) that have a mathematic closed-form solution; these models describe changes in a system, such as the thermal behavior of the ground when freezing or thawing occurs. Analytic equations can be validated and calibrated with empirical observations, as seen in the Kudryavtsev model that serves as an alternative to the Stefan model (Kudryavtsev et al., 1974). Meanwhile, equilibrium models are process- and physics-based models that define equilibrium permafrost conditions for a given annual regime by assuming a stationary temperature and snow cover climate; variations in either of these assumptions produce a range of mean annual ground temperatures (MAGTs) that cause permafrost conditions to deviate from equilibrium (Riseborough, 2007; Riseborough et al., 2008). Examples of equilibrium models include the Frost Number model (Nelson, 1986), TTOP model (Smith and Riseborough, 1996), and variations of the Kudryavtsev model (Anisimov et al., 1997).

More recent modeling efforts have adopted numerical and evidence-based approaches. Similar to equilibrium models, numerical models are also physics-based and are a type of mathematical model that relies on computational techniques to represent the behavior of a process over time. For example, numerical models can simulate the evolution of permafrost and ground thermal regimes over continental and decadal scales (Riseborough et al., 2008). Lastly, evidence-based models are mathematical models based on a set of statistical and probabilistic assumptions that were made on a particular variable and process of interest. Examples of statistical models include an analysis of the relationship between MAGT and ALT developed by Aalto et al. (2018), a permafrost infrastructure hazard assessment developed by Hjort et al. (2018), and an evaluation of the spatial and temporal influence of shrub expansion on frost table depth developed by Wilcox et al. (2019). Table 1 compares the input and output parameters of select permafrost models.

There are advantages and disadvantages to every model development approach. For instance, while analytical models can provide

closed-form solutions based on mathematical representations, they typically do not integrate site-specific, real-world conditions such as snow cover time series (Riseborough et al., 2008). Conversely, numerical models typically can address this limitation, but they require the input of spatial data to set up initial conditions and subsequent model spin up; this can be an issue, as data are not always readily available to initialize every model component (Biskaborn et al., 2015; Gruber, 2012; Serreze and Barry, 2014). In these cases, modelers revert to alternative mathematical representations or parameterizations and/or do not fully validate their models (Gruber, 2012; Riseborough et al., 2008). In the permafrost modeling realm, the representation of ground thermal regime and/or vegetation dynamics can be very limited. Other key limitations include those inherent to the chosen modeling approach adopted, and data variability (Lawrence et al., 2008; Riseborough et al., 2008; Tao et al., 2017). Along those lines, the models can provide as confident predictions as good as the data available to calibrate them and test them; in the case of permafrost, there remains large uncertainties that pertain to permafrost distribution, thickness, and ice content, among many more (Gruber, 2012; Hugelius et al., 2020).

Permafrost models commonly include the following input parameters (Table 1): air temperature, precipitation (particularly snow cover and/or depth), soil temperature, and soil moisture. Vegetation cover, topography, and soil texture are less common, albeit important additions. A difficulty in assessing permafrost model performance and representation is that most model simulations are conducted in Alaska (e.g., Debolskiy et al. (2020), Jafarov et al. (2012), Nicolsky and Romanovsky (2018), Pastick et al. (2015), and Wang et al. (2020)), as that is where there are the most and highest quality observations that allow for model calibration (Biskaborn et al., 2015). By limiting the spatial domain for model development and/or testing, it is possible that models may not be applicable to other regions, such as Canada or Siberia. While improving existing models and modeling approaches is important work, it is possible that an alternative type of model – one that would allow for the integration of different data types and a novel representation of permafrost thaw dynamics – would provide the community with new benchmarks against which to compare and contrast model outputs.

2.2. Bayesian methods

A BN framework has the potential to combine physics- and empirically-based modeling approaches with statistics and probability in order to link various components of a system (e.g., the Arctic) together and make predictions (e.g., permafrost thaw depth). The framework allows for the integration of multiple types of evidence, such as observations, model outputs, and expert assessments. This integration of evidence may help address the limitations and gaps of current permafrost models. The model also quantifies uncertainties pertaining to each variable on the predictions of future permafrost thaw. Further, this modeling approach is transparent in that the interactions between variables in the BN are explicitly represented. Few studies have utilized Bayesian methods to assess environmental changes in the Arctic (e.g., Qin et al. (2018) and Wainwright et al. (2017)), and the most comprehensive Arctic BN study only includes evidence in the form of expert assessment (Webster and McLaughlin, 2014). Our research expands upon these studies and includes a comparison of the PermaBN results to in situ observations.

BNs are probabilistic and cause-effect networks; they are constructed to represent variables ("nodes") and the relationships ("arcs") between these variables. Variables may be classified as "parent" (cause) or "child" (effect) nodes. Variables can also be further classified by their "type," such as "decision" or "chance" nodes. Decision nodes are those that are non-random or non-variable (e.g., topographic aspect), while chance nodes are those that have a random component to them (e.g., air temperature). A number of "states" can be attributed to each node; these states are typically represented as categories that capture the current state the variable is in and the states that the variable can shift to. For instance, a variable may exist in a low, medium, or high state. Decision nodes do not have probabilities associated with them, and the user sets the states (i.e., is given choices). The inclusion of decision nodes aids in the exploratory analysis of different scenarios. For chance nodes, on the other hand, a probability is assigned to each one of these states based on existing evidence, such as physical observations, model outputs, or expert assessment. The use of BN's become optimal when the complexity of the problem escapes either available physics or the association (not causation) of empirical formulation (e.g. regression).

BNs are based on a specific case of Bayes' theorem that describes the probability of an event given prior conditions and how beliefs change to account for new evidence (Korb and Nicholson, 2004). The concept of Bayesian inference is formalized in the equation:

$$P(H|E) = \frac{P(E|H)P(H)}{P(E)}$$

where the probability of a hypothesis H given some evidence E is equal to its likelihood $P(E|H)$ times its probability prior to any evidence $P(H)$, normalized by the probability of the evidence $P(E)$ being true (Korb and Nicholson, 2004). A graphical representation of the causal relationship between H and E is seen in Fig. 1.

An 'informed and simple synthetic' case study containing three chance nodes (air temperature, soil temperature, and thaw depth) is used to illustrate the theoretical background of a BN (Fig. 2). In this model, air temperature (a parent node) influences soil temperature (a child node), with the latter then impacting thaw depth (also a child node). Parentless nodes (e.g., air temperature) are quantified by marginal probabilities. Assume that it is known from either physical observations, model outputs, or expert assessment that air temperature has a 75% marginal probability of being low, 15% probability of being medium, and 10% probability of being high. These probability values can be estimated (a) directly from historic datasets based on physical observations of the variable of interest when translated into relative frequency statistics via an empirical cumulative distribution function (when data are sufficient); (b) from model outputs that allow the estimation of first and second order statistics to define probability distribution models that allow for the estimation of probabilities (when limited data are available); and (c) from experts' assessments, when knowledge is translated into probability values (when no data at all are available). Arcs on the other hand represent the causal dependencies between nodes and help build the conditional probability tables (CPTs) that link a parent node to a child node; a node is considered 'informed' when its CPT is determined by evidence. In a BN with n nodes, $\boldsymbol{X_1 \ldots X_n}$, the joint distribution is represented by $\boldsymbol{P(X_1 = x_1, X_2 = x_2, \ldots, X_n = x_n)}$, or $\boldsymbol{P(x_1, x_2, \ldots, x_n)}$. Using the chain rule of probability theory, this factorizes to $\boldsymbol{P}(x_1, x_2, \ldots, x_n) = \boldsymbol{P}(x_1) \times \boldsymbol{P}(x_2|x_1) \ldots, \times \boldsymbol{P}(x_n|x_1, \ldots, x_{n-1}) = \prod_i \boldsymbol{P}(x_i|x_1, \ldots, x_{i-1})$; when the value of a particular node is conditional only on the values of the parent nodes, this reduces to $\boldsymbol{P}(x_1, x_2, \ldots, x_n) = \prod_i \boldsymbol{P}(x_i|\boldsymbol{Parents}(X_i))$ (Korb and Nicholson, 2004).

In the Fig. 2 example, the arc between air temperature and soil temperature builds the soil temperature CPT, and the arc between soil temperature and thaw depth builds the thaw depth CPT. The method for determining the low, medium, or high state probabilities P(E) of a node depends on the particular type of evidence being used to inform the BN. In the case of evidence from physical observations (typically when data are sufficient), one could use historic data to build empirical cumulative distribution functions and use these to map the low, medium, and high range classifiers (e.g., by setting thresholds along the variable of interest, and then using the cumulative density function to define the probability estimates falling between low, medium, and high). The same approach would be used to determine the conditional probabilities P(H_1|E) and P(H_2|H_1); the CPTs would be determined by how many observations fall into each set of states (e.g., the probability of there being

Table 1
Table of select permafrost models detailing their model type classification, select input parameters, and outputs.

Model Name and Reference	Type	Inputs										Outputs
		Air Temperature	Aspect	Ground Temperature	Precipitation	Snow Depth	Soil Density	Soil Water Content	Solar Radiation	Thermal Conductivity	Vegetation Height	
Frost Number (Nelson, 1986)	EQ	X			X	X		X		X		Depth of frost; surface frost number
TTOP (Smith and Riseborough, 1996)	EQ	X		X						X		Mean annual temperature at base of active layer
Kudryavtsev (Anisimov et al., 1997, Kudryavtsev et al., 1974)	EQ; A - EM	X		X		X	X	X		X	X	Depth of seasonal freezing/ thawing
One-dimensional finite-difference model (Goodrich, 1978, Goodrich, 1982)	N					X	X	X		X		Position of freezing/thawing interface
Northern Ecosystem Soil Temperature (NEST) (Zhang et al., 2006)	N	X			X		X		X	X	X	ALT; depth to permafrost table
GIPL2-MPI (Jafarov et al., 2012)	N	X		X	X	X		X		X		MAGT; ALT
Catchment Land Surface Model (CLSM) (Tao et al., 2017)	N	X		X	X				X	X	X	ALT; soil temperature profile
Numerical Experiments by Nicolsky and Romanovsky (2018)	N			X			X	X		X		Rate of permafrost thaw
Stefan model (Lunardini, 1981)	A	X								X		Phase change boundary
N Factors (Lunardini, 1978)	EM	X		X								n-factor
Frost Index (Nelson and Outcalt, 1987)	EQ; EM	X		X	X	X	X	X		X		Stefan frost number
PERMAKART (Keller, 1992)	S - EM	X	X	X		X			X			Map of permafrost distribution
Aalto et al. (2018)	S	X			X				X			MAGT; ALT
Hjort et al. (2018)	S			X			X					Geohazard indices
Wilcox et al. (2019)	S		X			X					X	Quantification of micro-scale variables on frost table depth

Ten of the most common input parameters were selected for comparison, with an "X" denoting if a model includes that input parameter. Type abbreviations: EQ (equilibrium), A (analytical), N (numerical), EM (empirical), S (statistical).

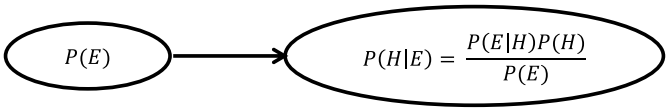

Fig. 1. Graphical (BN) representation of the casual relationship between the hypothesis (H) and evidence (E) as probabilities (P). Note that there could be multiple parent nodes. Adapted from Varela Gonzalez (2017).

low soil temperature when there is low air temperature and low thaw depth when there is high soil temperature). In the case of using evidence from model outputs (typically when limited data are available), probabilities can be estimated by using models (e.g., physically-based like models based on the laws of thermodynamics, or empirically-based like regression or artificial intelligence) that simulate scenarios of the variable of interest, which simulations allow for the estimation of first and second order statistics to define a probability distribution model from which estimation of probabilities can be computed. In the case of using experts' assessments (typically when no data at all are available), knowledge is then translated into probability values, for instance, knowledge that air temperatures are very likely to be low while the likelihood of air temperature being medium is only slightly greater than the likelihood of air temperature being high. When using any of the evidence types to produce probability values to support the model's nodes, the effort is focused in 'sampling' reality to capture first the general trend (expectation), and then the associated uncertainty (variance). Therefore, it is anticipated that the more sampling of available

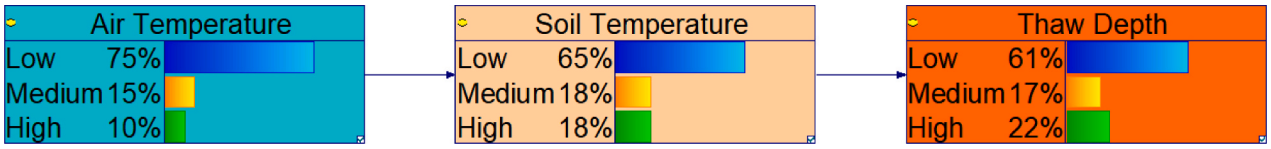

Air Temperature P(E)	
Low	0.75
Medium	0.15
High	0.10

$P(H_1\|E)$		Air Temperature P(E)		
		Low	Medium	High
Soil Temperature $P(H_1)$	Low	0.80	0.25	0.10
	Medium	0.10	0.60	0.10
	High	0.10	0.15	0.80

$$[0.75 \quad 0.15 \quad 0.10]^T \begin{bmatrix} 0.80 & 0.25 & 0.10 \\ 0.10 & 0.60 & 0.10 \\ 0.10 & 0.15 & 0.80 \end{bmatrix} = \begin{bmatrix} (0.75*0.80)+(0.15*.25)+(0.10*0.10) \\ (0.75*0.10)+(0.15*0.60)+(0.10*0.10) \\ (0.75*0.10)+(0.15*0.15)+(0.10*0.80) \end{bmatrix}$$

$$= \begin{bmatrix} 0.6475 \\ 0.175 \\ 0.1775 \end{bmatrix}$$

Soil Temperature $P(H_1)$	
Low	0.65
Medium	0.18
High	0.18

$P(H_2\|H_1)$		Soil Temperature $P(H_1)$		
		Low	Medium	High
Thaw Depth $P(H_2)$	Low	0.85	0.25	0.10
	Medium	0.10	0.50	0.10
	High	0.05	0.25	0.80

$$[0.65 \quad 0.18 \quad 0.18]^T \begin{bmatrix} 0.85 & 0.25 & 0.10 \\ 0.10 & 0.50 & 0.10 \\ 0.05 & 0.25 & 0.80 \end{bmatrix} = \begin{bmatrix} (0.65*0.85)+(0.18*0.25)+(0.18*0.10) \\ (0.65*0.10)+(0.18*0.50)+(0.18*0.10) \\ (0.65*0.05)+(0.18*0.25)+(0.18*0.80) \end{bmatrix}$$

$$= \begin{bmatrix} 0.6155 \\ 0.173 \\ 0.2215 \end{bmatrix}$$

Fig. 2. A simple BN with three chance nodes: air temperature, soil temperature, and thaw depth. Probabilities represent synthetic, illustrative cases of the marginal (air temperature) and joint (soil temperature and thaw depth) probabilities. Tables show the marginal (or conditional) probabilities followed by the equations calculating the joint probabilities.

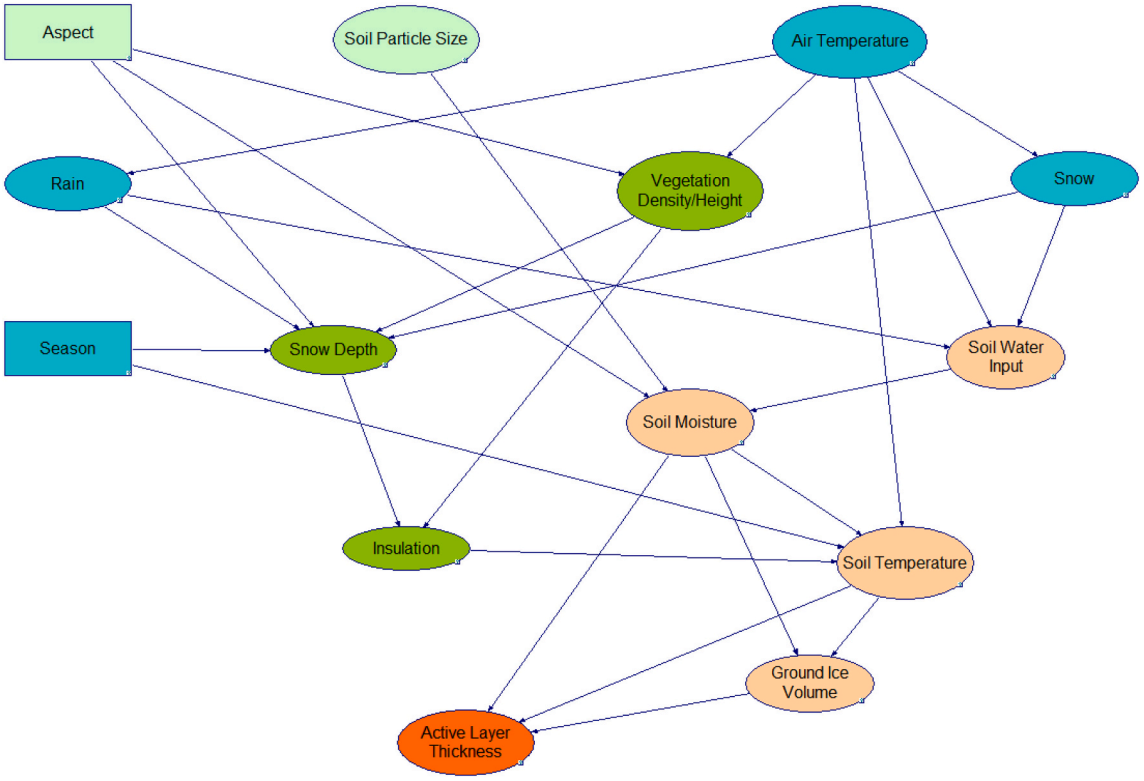

Fig. 3. Pre-validation (i.e., preliminary) conceptual model, which includes 14 nodes, 26 arcs, and 43 states. Geological variables are represented in light green, atmospheric variables in teal, surface insulation variables in dark green, soil variables in light orange, and ALT in dark orange. Decision nodes are represented as boxes; chance nodes are ovals. For a list of causal relationships and their corresponding references, refer to Beall (2021). (For interpretation of the references to color in this figure legend, the reader is referred to the web version of this article.)

physical observations, of model outputs, and of experts' knowledge, the better definition of the variable's trend and reduction of its uncertainty, where both have a significant impact on the prediction of the BN.

While the probabilities provide a quantification of the relationships between variables, the topology of the network captures qualitative relationships between the variables (Aguilera et al., 2011; Korb and Nicholson, 2004). It is important to note that BNs are directed acyclic graphs, meaning that nodes and arcs cannot be connected in a directly cyclic manner. As such, the relationships between nodes and arcs represent the causal evidence for a process that cascades through the model, from parent to children, in a cause-effect manner, within a given "step" in space and time. Similar problems have been addressed following this approach, from natural resource management, to the integration of remote sensing data with physically-based landslide models, to the design of environmental friendly drilling systems, and early warning systems (Al-Yami et al., 2010; Das et al., 2019; Fox et al., 2017; Medina-Cetina and Nadim, 2008; Yu et al., 2012). Within each model step, feedbacks are not allowed between nodes. For instance, if high thaw depth is considered a proxy for carbon release, an arc from thaw depth to air temperature cannot be made to represent the effects of increased carbon release on air temperature. Instead, the BN model would have to be run again with updated marginal probabilities for air temperature to reflect the new increased carbon conditions. Alternatively, a "dynamic" BN could be used to represent feedbacks (Chen and Pollino, 2012; Kjaerulff, 1995).

A primary advantage to using a BN approach is the ability to incorporate three types of evidence (i.e., observations, model outputs, and expert assessments) into a single model. This is particularly helpful to represent the Arctic system, as available evidence may be regionally limited, incomplete, or inexistent. The BN approach is fully transparent, departing from modeling methods based on black-boxes. In addition, uncertainties in the model and the system are expressed through the distribution of probabilities assigned to each node state, and the node's information content is propagated through the network to the final model endpoint following the Markovian principle, which allows for the estimation of each node's probability density function (Korb and Nicholson, 2004). Lastly, by employing the principle of Occam's Razor, BNs may be more suitable than other modeling approaches for scenarios where it is important to engage stakeholders in the modeling process of a system (Pearl, 2009). Keeping the BN as simple as possible is also necessary for maintaining sensitivity of outputs to inputs, and for avoiding additional uncertainty propagation in the model. Despite appearing simpler than other models, BNs are well suited for modeling complex systems with a large number of variables (Getoor et al., 2004) or being integrated into larger models (Chen and Pollino, 2012). Another unique advantage to BNs is their capability for both forward (prognosis/cause to effect) and inverse (diagnosis/effect to cause) modeling. Examples of Fig. 2 in prognosis and diagnosis mode can be seen in Beall (2021).

As with all methodologies, there are known limitations to the BN approach. One such limitation is that development of BNs is hindered by the lack of a universally accepted methodology to develop them (Weber et al., 2012), and the validation of reliable expert elicitation is a known challenge (Kaikkonen et al., 2021; Uusitalo, 2007). Another limitation arises when experts must validate the model; the size of a node's CPT increases $S\prod_{i=1}^{n} P_i$ where S=the number of states and P_i=the number of states in the ith parent node (Marcot et al., 2006), meaning that limiting the size of the node's CPT is especially important in BNs where CPTs are defined through expert assessment since the CPT can quickly become too large for the human brain to adequately comprehend. Despite these limitations, the unique advantages of this approach hold great potential for application to the environmental sciences (Kaikkonen et al., 2021; McLaughlin and Packalen, 2021; Qin et al., 2018; Wainwright et al.,

Table 2
Definition of nodes and associated possible states included in the pre-validation (i.e., preliminary) version of PermaBN.

Node	Type	Definition	States
Active Layer Thickness	Chance	The depth/thickness of the layer of ground subject to annual thawing and freezing in areas underlain by permafrost	Low, Medium, High
Air Temperature	Chance	Temperature of the air near the surface of the Earth based on 2081–2100 RCP future warming projections	RCP 2.6, RCP 4.5, RCP 8.5
Aspect	Decision	The arrangement of the natural and artificial physical features of an area, or more particularly, the aspect, or positioning of a feature in a specified direction	North, East, South, West
Ground Ice Volume	Chance	Volume of all types of ice contained in freezing and frozen ground, which includes bedrock, sediment, organic matter, and water	Low, Medium, High
Insulation	Chance	The state of something being insulated, or protection of something by interposing material that prevents the loss of heat	Low, Medium, High
Rain	Chance	Moisture condensed from the atmosphere that falls visibly in separate drops	Low, Medium, High
Season	Decision	Division of the year marked by the presence or absence of snow	Snow Free, Snow
Snow	Chance	Atmospheric water vapor frozen into ice crystals and falling in light white flakes or lying on the ground as a white layer	Low, Medium, High
Snow Depth	Chance	Measurement of snow that has fallen during previous weather events	Low, Medium, High
Soil Moisture	Chance	Water that is held in the pore spaces between soil particles	Low, Medium, High
Soil Particle Size	Chance	Composition of mineral soil by relative soil particle size	Clay, Silt, Sand
Soil Temperature	Chance	Measurement of the warmth of the soil	Low, Medium, High
Soil Water Input	Chance	The ratio of precipitation to evaporation	Low, Medium, High
Vegetation Density/ Height	Chance	Percentage of soil which is covered by green vegetation, or height of the dominant vegetation classes	Low, Medium, High

2017).

So far, the most comprehensive use of a BN in the context of the Arctic and permafrost is a study by Webster and McLaughlin (2014) that assesses the vulnerability of permafrost to thaw and estimates the impacts of permafrost thaw on greenhouse gas (GHG) emissions and climate feedbacks in the Canadian Arctic and Hudson Plain regions using a Bayesian Belief Network (BBN). The objective of the study was to create a tool that aids policymakers in understanding the vulnerability of permafrost to thaw and resulting carbon emissions (Webster and McLaughlin, 2014). The BBN is arranged in a hierarchical manner to reflect the vulnerability assessment components of sensitivity, exposure, and adaptive capacity; however, the adaptive capacity component is not explicitly represented in the version of the model presented in the study. Nodes in the BBN represent the themes of future and current mean annual air temperature and ground conditions, heat transfer, carbon susceptibility, permafrost thaw, GHGs, and feedback to climate change. Although BNs are capable of integrating various types of evidence, the study by Webster and McLaughlin (2014) only included evidence from expert assessment. It is arguable that their findings could have been augmented by the integration of observational data and/or model outputs, as the authors recognize that the expert assessment approach can lead to accurate, but not necessarily precise, predictions. That said, their study is a convincing example of how observational data are not a limitation to generating useful predictions of permafrost thaw; it also demonstrated the usefulness of BBNs as potential policy tools, as the model allows for various future scenarios and consequences to be analyzed. The expectation is that as observations and model outputs become available, estimates of the model become more accurate and precise when added to the experts' assessments.

3. PermaBN development and methods

3.1. PermaBN components

The following subsections define and review the key geomorphic and ecological processes that influence continuous permafrost thaw and that are represented in PermaBN; while it is acknowledged that hydrological processes such as river dynamics and the presence of surface water (e.g., lakes) also exert an important control on permafrost thaw (Burn and Kokelj, 2009; Kokelj and Jorgenson, 2013; Zheng et al., 2019), PermaBN, along with the majority of existing permafrost models (e.g., Kudryavtsev model by Anisimov et al. (1997), GIPL2-MPI by Jafarov et al. (2012), and Catchment Land Surface Model (CLSM) by Tao et al. (2017)), implicitly include hydrological processes through the representation of ground heat fluxes and thermal conductivity:

(1) Topography: landscape-scale geologic and topographic characteristics and processes typically remain consistent, at the human timescale, in their influence on other system components such as vegetation communities, snow depth, and soil moisture. As such, local topography can influence snow distribution, incident radiation, and wind exposure, which can impact soil moisture and soil temperature (Aalto et al., 2013; Serreze and Barry, 2014; Young et al., 1997). In the northern hemisphere, northerly aspects tend to be snowier, cooler, and receive less intense incoming radiation than southerly aspects (Evans et al., 1989; Petzold and Mulhern, 1987; Wilcox et al., 2019). The effects of aspect on radiation are lessened at higher latitudes, particularly for east and west aspects (Holland and Steyn, 1975). Nonetheless, the differences between north and south slopes can still be significant (e.g., Evans et al. (1989) and Myers-Smith et al. (2020)).
(2) Soil texture and density: the effects of soil particle size and density on soil moisture and soil temperature are considered. Soil particle size (or texture), influences soil moisture by controlling the moisture retention rate and thermal conductivity of the soil (Arya and Paris, 1981; Young et al., 1997). For instance, finer particles such as clay can retain more moisture than coarser particles such as sand (Meentemeyer and Zippin, 1981). Soil texture can also be considered from the perspective of soil bulk (dry) density. In this case, a sandy soil has a higher dry density than a silty or clayey soil; organic soils generally have very low dry densities (Abu-Hamdeh and Reeder, 2000). Dry bulk density influences soil thermal conductivity, such that an increase in density at a given soil moisture content increases the thermal conductivity of that soil (Abu-Hamdeh and Reeder, 2000). Thermal conductivity therefore tends to be highest in sandy (i.e., high bulk density) soils and lowest in organic (i.e., low bulk density) soils. Lastly, sandy soils have a high infiltration rate, but low available water content, while clayey and organic soils have the highest volumetric water contents (Abu-Hamdeh and Reeder, 2000).
(3) Surface air temperature and precipitation regimes: these atmospheric variables exert direct and important influences on soil and vegetation properties. For instance, warmer surface air

Table 3
Complete list of changes made to the pre-validation (i.e., preliminary) model during validation of PermaBN with explanations for why each change was made.

Pre-validation model component	Validation model refinement	Explanation
Node: Active Layer Thickness	Node renamed to "Thaw Depth"	"Thaw Depth" allows for a more accurate interpretation of the node in the context of the seasonal dynamics represented in the model. In other words, "Active Layer Thickness" only refers to a certain portion of the permafrost profile that thaws in the summer, and a more inclusive term was desired.
Node: Ground Ice Volume	Node renamed to "Active Layer Ice Content"	"Active Layer Ice Content" better reflects an underlying assumption that ground ice is limited to the upper layer of the soil column.
Node: Soil Particle Size	Node renamed and redefined to "Soil Density"	"Soil Particle Size" only accounted for the mineral soil states of sand, silt, or clay and their respective moisture retention properties. "Soil Density" accounts for both the effects of mineral soil particle size and soil organic content on moisture retention and thermal conductivity. With the renamed node, the states are also redefined from "Sand," "Silt," and "Clay" to "Low," "Medium," and "High" to account for both the consideration of soil organic content and consistency in model terminology.
Node: Vegetation Density/Height	Node renamed to "Vegetation Height"	"Vegetation Height" is the variable that is more often reported in physical observation datasets or in the literature.
Node States: Air Temperature	Node states redefined from three RCP scenarios to "Low," "Medium," and "High"	Defining the node states as simply "Low," "Medium," and "High" enhances the consistency of terminology used in the model as well as generalizes the node for use with physical observations or other model scenarios.
Node arc: Insulation	New arc added between "Soil Density" and "Insulation"	This new arc allows for representation of the effects of soil organic content on moisture retention, thermal conductivity, and insulation to be accounted for.
CPT: Insulation	The CPT values of the Insulation node were adjusted	Adjustements were necessary after redefining "Soil Particle Size" to "Soil Density."
CPT: Soil Moisture	The CPT values of the Soil Moisture node were adjusted	Adjustments were necessary after redefining "Soil Particle Size" to "Soil Density." While modifying the CPT values, an error was also found where soil moisture conditions for certain aspects under low soil water input conditions were swapped.
CPT: Soil Temperature	The CPT values of the Soil Temperature node were adjusted	Further investigation suggested that there is a positive relationship between soil moisture and soil temperature in the snow season (i.e., higher soil moisture leads to warmer temperatures) and a negative relationship in the snow free season (i.e., higher moisture leads to cooler temperatures); see Beall (2021) for details.
Graphical Structure	Reorganization of the BN into a tiered structure	The model was graphically reorganized to emphasize the cause-effect nature of the model. For instance, it becomes easier to see the distinct tiers (parent nodes at the top, intermediate child nodes in the middle, and the response of the system at the bottom) in the model.
Assessment of Nodes During Experiments	At least 75% (i.e., 9 out of 12) chance nodes had to respond as expected to the prognosis and diagnosis experiments	A qualitative assessment of node behavior was introduced to enhance robustness of the model and allow for further adjustment of the node CPTs prior to informing the model with physical observations from a case study. Whether or not a node responded as expected was dependent on (a) expected conditions gathered from the literature (e.g., higher chance of rain than snow under warmer conditions) and (b) trends in the node response as opposed to the magnitudes of the response.

temperatures increase the length of the growing season, which may contribute to shrub expansion and increased photosynthetic activity across the tundra (Myers-Smith et al., 2011; Myers-Smith et al., 2020). Likewise, the relationship between increased surface air temperatures and increased soil temperatures is well documented (Boike et al., 2003; Oelke and Zhang, 2004; Park et al., 2014; Zhang et al., 2018). Many studies have also identified surface characteristics that work to modulate the relationship between air and soil temperatures, such as the insulation properties of snow and water cover (Kokelj and Jorgenson, 2013; Zhang et al., 2018). As for precipitation, atmospheric air temperatures affect the ratio of precipitation that falls as rain vs. snow, and as temperatures continue to warm, a higher ratio of precipitation falling as rain is expected across the Arctic (Bintanja and Andry, 2017). A higher ratio of rainfall would also impact snow depths by melting existing snow cover (Boike et al., 2003; Screen and Simmonds, 2012). As for precipitation regimes, the Arctic is expected to experience increased precipitation totals throughout the 21st century (Bintanja and Andry, 2017), with decreased amounts of snow. Lastly, air temperature and precipitation modulate soil moisture, primarily through snowmelt and rainfall, as well as evaporative processes (Rouse et al., 1997; Young et al., 1997).

(4) Biota: vegetation height has known influences on ground insulation via shading in the summer and increased snow depth in the winter (Grunberg et al., 2020; Myers-Smith et al., 2011; Wilcox et al., 2019), with implications for soil temperatures and permafrost thaw depths. In winter, increased vegetation density and height have been shown to locally increase snow depths by trapping snow in branches (Gockede et al., 2019; Grunberg et al., 2020; Myers-Smith et al., 2011; Wilcox et al., 2019), and the insulation properties of snow contribute to warmer winter soil temperatures (Gockede et al., 2019; Myers-Smith et al., 2011; Park et al., 2014; Zhang et al., 2018). This slows down, or prevents, the active layer from refreezing during the cold season (Jan and Painter, 2020; Zhang et al., 1996). In the summer, vegetation cover shades the ground and reduces the thermal gradient into the ground, thereby leading to cooler summer soil temperatures and reduced active layer depths (Aalto et al., 2013; Blok et al., 2010; Grunberg et al., 2020; Myers-Smith et al., 2011; Young et al., 1997). Some studies suggest that vegetation shading may help protect permafrost from thaw by offsetting some of the influences of increased air temperatures (Blok et al., 2010), though others argue that the warming-induced increase in shrub cover will ultimately offset the local cooling influence due to surface albedo changes related to the protrusion of shrub stems above the spring snowpack that lead to warmer soil temperatures and deeper active layers (Lawrence and Swenson, 2011). In this latter case, the vulnerability of permafrost to thaw could be increased.

(5) Soil temperature and moisture: soil thermal dynamics are affected by moisture (Oelke and Zhang, 2004; Zwieback et al., 2019). Increased soil moisture, which would be more characteristic of lower bulk density (i.e., organic or clayey), typically leads to decreased soil temperatures since it increases heat capacity, and evaporation consumes a large amount of energy. However, soil moisture and high bulk density also increase the thermal conductivity of soil, allowing heat to penetrate the ground more effectively and increase active layer depths (Frauenfeld et al.,

2004). Many recent studies suggest that the influence of soil moisture is stronger on thermal conductivity than on conductive heat transfers, though this influence may not hold at deeper soil depths and in continuous permafrost areas that have a higher concentration of mineral soils (Douglas et al., 2020; Fisher et al., 2016; Loranty et al., 2018). As for the relationship between soil temperature and permafrost thaw, it is well established. Increased soil temperatures lead to increased active layer thickness (ALT) through increases in the ground heat flux (Frauenfeld et al., 2004; Liljedahl et al., 2016; Loranty et al., 2018; Schuur and Mack, 2018).

(6) Ground ice content within the active layer: similar to permafrost, ground ice is vulnerable to degradation as a result of increased soil temperatures (Jorgenson et al., 2015; Liljedahl et al., 2016). While soil moisture is a critical variable in ground ice growth, with wet sites more likely to have high ice concentrations than dry sites (Meentemeyer and Zippin, 1981; O'Neill and Burn, 2012), the presence of ground ice can help delay active layer thickening due to the large amount of latent heat required to melt the ice (Jorgenson et al., 2015; Lee et al., 2014; Loranty et al., 2018; Schuur and Mack, 2018). Conversely, high ground ice content can lead to pronounced ground subsidence when that ice melts, further promoting permafrost thaw (Jorgenson et al., 2015; Kokelj and Jorgenson, 2013).

3.2. PermaBN development

The objectives of PermaBN are to: (1) provide an alternative permafrost modeling framework that improves understanding and prediction of permafrost dynamics under various climate or ecosystem conditions (i.e., provide a method that allows for exploratory and scenario analysis), (2) identify knowledge and data gaps that hinder our understanding (and modeling capabilities) of permafrost dynamics, and (3) facilitate participatory modeling among researchers and/or stakeholders.

Following the best practices in BN modeling outlined by Medina-Cetina and Nadim (2008), Chen and Pollino (2012), and seen in works such as those by Fox et al. (2017), the model development process entails a series of critical steps: (1) defining model objectives and scope, (2) creating a conceptual model of the system to form the structure of the BN, (3) defining states and conditional probabilities of all variables, (4) evaluating the BN using a suite of both quantitative and qualitative model evaluation methods, and (5) documenting assumptions, uncertainties, descriptions and reasoning for each node and linkage, data and information sources, and evaluation of results.

In this proof-of-concept stage, the scope of PermaBN is limited to the prediction of permafrost thaw depth in the continuous permafrost region as a result of a handful of key terrestrial factors (see *PermaBN Components*). While the emphasis is limited to the geomorphic and ecological processes that influence permafrost thaw, future development of PermaBN could introduce hydrological factors (among others). Note that PermaBN was designed with a multiyear timescale in mind. In its current form, PermaBN is not meant to be viewed as a true environmental risk assessment model since it lacks the quantification of utility associated with the consequences of permafrost thaw. Instead, it should be viewed as a model aimed at predicting environmental impacts. Future development could use PermaBN as a sub-module that would be included into a comprehensive Arctic ecosystem risk framework. It should also be noted that, in its current form, PermaBN should not be applied to non-continuous or transitional permafrost regions due to differing drainage patterns, vegetation types, and ground temperature/permafrost relationships (Burn and Kokelj, 2009).

3.3. Model pre-validation

A preliminary conceptual model (Fig. 3) was created to form the structure of the BN. The “nodes” and “arcs” of PermaBN were represented using the software program GeNIe (BayesFusion, 2019). In the case of PermaBN, this graphical network represents a hypothesis about the terrestrial variables that control permafrost thaw depth. Multiple BNs could be created to reflect different hypotheses or spatiotemporal domains, if desired. In other words, PermaBN is by no means a unique or “be-all and end-all” representation; rather, it is the best initial attempt at representing the key terrestrial processes at play in permafrost thaw. Ultimately, the goals of the conceptual model are to provide a structure for the BN and identify the causal relationships across the system. In environmental BNs, node and arc selection and definition are typically determined through literature review or expert judgment (Kaikkonen et al., 2021). For this reason, the variables included here were determined primarily through extensive review of peer-reviewed scientific literature and collaboration with other researchers and scientists during two workshops that took place in 2019 at Texas A&M University.

The following variables were selected for the PermaBN model because they are thought to be most impactful on permafrost thaw: (1) geological setting (aspect and soil particle size), (2) atmospheric conditions (air temperature, rain, snow, and season), (3) surface insulation (vegetation density/height, snow depth, and insulation), and (4) soil properties (soil moisture, soil water input, soil temperature, and ground ice volume). ALT is the final variable in the network and is the response, or endpoint, of the system. Other variables, such as soil thermal conductivity, are implicit to the model through the causal relationships between nodes. For instance, soil particle size influences soil moisture and insulation, which are known to influence thermal conductivity, and hence, soil temperature. Similarly, some hydrological processes could be considered implicit to the soil moisture node (Woodard et al., 2021). For example, snow melt contributes to soil water input, and soil particle size controls infiltration rates, and hence, soil moisture content.

After characterizing each node and their associated states (Table 2), the CPTs for the nodes were determined; the maximum number of parent nodes for any node was limited to five to limit the size of the CPTs while still allowing for as many causal relationships to be explicitly represented as possible. It is ideal to include as much evidence as possible when creating the CPTs (Medina-Cetina and Nadim, 2008), but evidence can sometimes be sparse in environmental studies. In that case, the CPTs are derived through expert judgment. One method for initially determining the CPTs for any given node is to assign a uniform distribution; this is commonly the case if the variable conditions are unknown. CPT values can then be adjusted as necessary when evidence becomes available for the variable, whether it is from physical observations, model outputs, or expert assessments (Marcot et al., 2006). It is also common to initially determine the CPTs in a symmetric manner when using expert assessments as the evidence source (McLaughlin and Packalen, 2021). In a symmetric CPT, the probability of the “lowest” scenario would be equal to the probability of the “highest” scenario. In the pre-validation version of the PermaBN model, probability values were selected to represent trends rather than true probabilities of what may occur in reality; those trends were established on the basis of existing literature. For example, a high probability (60%) was given to the medium air temperature scenario, indicating the state of knowledge that it is more likely that a moderate amount of warming will occur in the Arctic over the coming decades as opposed to no/little warming or extreme warming; similarly, extreme warming is more likely than no/little warming (Meredith et al., 2019).

To test the accuracy or representativeness of the CPTs (Appendix A), 46 prognostic experiments (Appendix B) were designed to illustrate how

Table 4
Definition of nodes and associated possible states included in the expert assessment validation version of PermaBN. Changes from the pre-validation version are bolded.

Node	Type	Definition	States
Thaw Depth	Chance	**The depth/thickness of the layer of ground subject to annual thawing and freezing in areas underlain by permafrost**	Low, Medium, High
Air Temperature	Chance	**Temperature of the air near the surface of the Earth**	**Low, Medium, High**
Aspect	Decision	The arrangement of the natural and artificial physical features of an area, or more particularly, the aspect, or positioning of a feature in a specified direction	North, East, South, West
Active Layer Ice Content	Chance	**Volume of all types of ice contained in the upper portion of the soil column that is subject to annual thawing and freezing**	Low, Medium, High
Insulation	Chance	The state of something being insulated, or protection of something by interposing material that prevents the loss of heat	Low, Medium, High
Rain	Chance	Moisture condensed from the atmosphere that falls visibly in separate drops	Low, Medium, High
Season	Decision	Division of the year marked by the presence or absence of snow	Snow Free, Snow
Snow	Chance	Atmospheric water vapor frozen into ice crystals and falling in light white flakes or lying on the ground as a white layer	Low, Medium, High
Snow Depth	Chance	Measurement of snow that has fallen during previous weather events	Low, Medium, High
Soil Moisture	Chance	Water that is held in the pore spaces between soil particles	Low, Medium, High
Soil Density	Chance	**Organic and mineral composition of soil per the measure of the amount of dry solid particles per unit volume**	**Low, Medium, High**
Soil Temperature	Chance	Measurement of the warmth of the soil	Low, Medium, High
Soil Water Input	Chance	The ratio of precipitation to evaporation	Low, Medium, High
Vegetation Height	Chance	**Height of the dominant vegetation classes**	Low, Medium, High

the incorporation of evidence affected children nodes in the model, particularly the model endpoint (prediction of ALT). The first set of experiments was conducted on a model where all the nodes were set to a uniform distribution (Appendix B). Then, informed nodes at varying levels of the model were introduced (Appendix B). The final set of experiments was conducted on a model where all the nodes were informed. In each of the experiment sets, a combination of the primary parent nodes (i.e., those nodes with no preceding nodes or incoming arcs) were set to the extreme scenarios that could be encountered in the system (e.g., low air temperatures, solar radiation, and soil particle size or high air temperatures, solar radiation, and soil particle size). A set of 13 diagnostic experiments (Appendix B) was also designed to check for consistency in the model. In contrast to the prognosis experiments, these effect-to-cause experiments focused on setting the response variable (ALT) to each of its states in a fully informed model to see if the parent node distributions responded as expected. Some of the diagnostic experiments also set intermediate parent nodes to different states to assess whether a node seems to be a primary driver of change in the model.

Collectively, these prognostic and diagnostic experiments represent the process of pre-validation (Medina-Cetina and Nadim, 2008). It allows for a check on the consistency of the model at the lower and upper bounds; for instance, if thaw depth does not respond as expected given the state of the parent nodes in the prognostic experiments, it is possible that: (1) the CPTs may not be well defined, and/or (2) the variables and connections between them may not sufficiently represent the process of permafrost thaw. In the event of the former, the CPTs simply need to be adjusted through further expert judgment, or ideally, through the incorporation of physical observations or model outputs. In the event of the latter, the model may need to be redesigned. When the system responds as expected per the modeler's judgment, the model can be considered pre-validated, and the results can be used for further validation of the model. All results of the pre-validation prognosis and diagnosis experiments can be found in Appendix B.

3.4. Validation – expert assessment

After pre-validation, the model moved into the validation stage. Here, validation first entailed meeting with a group of four experts at Texas A&M University to review the conceptual model and the results of the prognostic and diagnostic experiments. This validation stage is a fairly unique attribute of the PermaBN model development process, as most BN studies exclude validation from the development process (Aguilera et al., 2011; Kaikkonen et al., 2021). Of the studies that do conduct validation, the most common method for doing so is through expert assessment (Kaikkonen et al., 2021). Since the experts were familiar with both Arctic climates and introductory Bayesian modeling principles, only a brief overview of the current state of permafrost modeling research and of the statistical methods behind the two types of experiments was provided. The feedback and suggestions from the validation session were then used to refine the BN conceptual model. Refinements included: (1) renaming or redefining of nodes in the pre-validation conceptual model, (2) adjustment of soil moisture and soil temperature seasonal relationships, and (3) implementing a qualitative threshold for passing the CPTs defined in the pre-validation prognosis and diagnosis experiments see Table 3 for a complete list of changes and the corresponding explanations for each change. Table 4 provides an updated table of nodes, node definitions, and node states included in the validated PermaBN model, and Fig. 4 shows the updated conceptual model.

Before testing PermaBN with physical observations, the prognostic and diagnostic synthetic informed case study experiments were repeated with the updated conceptual model. The number of prognostic experiments was increased to 50, and the number of diagnostic experiments was increased to 32 in order to capture additional test cases pertaining to the endpoint node being the only informed node (Appendix B). Similar to the pre-validation experiments, the trend in the node responses was given higher priority than the magnitude of the response for determining whether the model responds as expected. If the extreme, fully informed prognosis and diagnosis experiments fail the qualitative validation method, then the nodes, their CPTs, and connections should be closely evaluated prior to informing the model with physical observations. Here, PermaBN passed the qualitative validation, and the updated model was used to evaluate model performance.

Key results of the validation prognosis experiments are as follows. In the completely non-informed, or uniform, model run, changing the states of any of the nodes did not result in a change in any of the other nodes (Appendix B). This is an illustration of the Bayesian principle of Markov conditions. The principle states that a node does not influence nodes that do not descend from it. Another way of stating this is that each node relies on what its prior nodes know. This principle is also illustrated in the experiments where only the four parent nodes are informed and, in many of the experiments, where only the uppermost children nodes are informed. For example, when only the air temperature and rain nodes are informed, rain will respond to changes in air temperature, but any children of rain will not exhibit any responses.

Similarly, if every node is informed except for thaw depth, the thaw depth node will not respond to changes in the parent nodes until it has been informed (Beall, 2021). That said, it is possible for children nodes

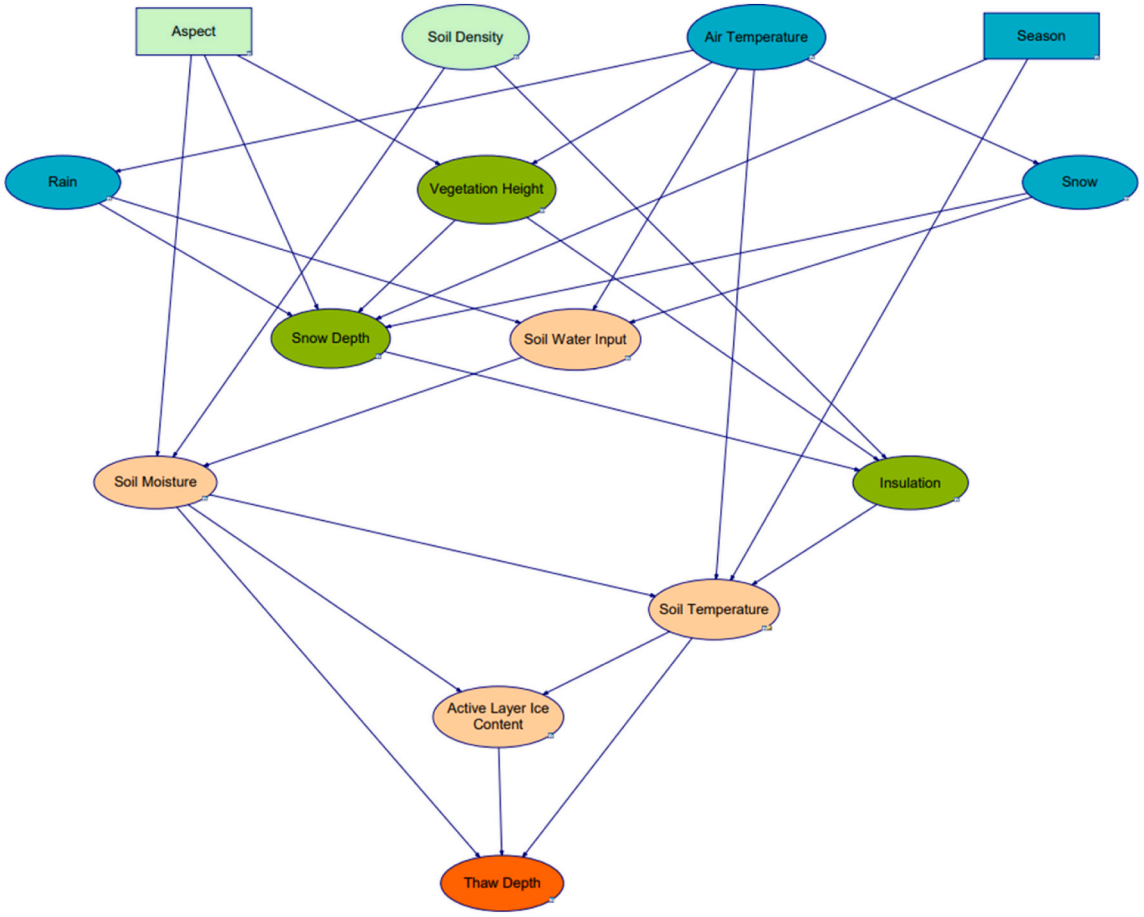

Fig. 4. PermaBN conceptual model after validation via expert assessment. In comparison to the pre-validation conceptual model, several nodes have been renamed, and an additional causal relationship has been added. There are now 27 arcs connecting the 14 nodes.

to respond if the child node and one or more of its prior nodes are informed. For instance, if the air and soil temperature nodes are informed, soil temperature will respond to changes in air temperature. However, if the insulation node is informed, it will still show a uniform conditional distribution since its parent nodes of vegetation density/height and snow depth are not informed. Thus, insulation will not affect soil temperature.

Increasing the number of informed nodes decreases the uncertainty in thaw depth predictions. Uncertainties in the model and the system are expressed through the distribution of probabilities assigned to each node state, and the uncertainties are propagated through the network to the final model endpoint (Chen and Pollino, 2012). In the experiments where all nodes except for soil temperature and snow depth were informed, thaw depth responded very little to changes in the primary parent nodes (Beall, 2021).

However, when soil temperature and snow depth were informed, thaw depth responded as expected to the low and high scenarios of the parent nodes. Fig. 5 shows the prognosis results for the low and high "extreme" scenarios of changes in thaw depth. In the case where aspect was set to north, soil density to low, air temperature to low, and season to snow, there was a high probability that thaw depth would be in a low state (Fig. 5A). This indicates a high probability that permafrost thaw would be low in scenarios promoting cooler temperatures and increased soil moisture. Similarly, in the case where aspect was set to south, soil density to high, air temperature to high, and the season to snow-free, there was a high probability that thaw depth would be in a high state (Fig. 5B). This indicated a high probability that permafrost thaw would be high in scenarios promoting warmer temperatures and decreased soil moisture. While the model responds as expected at this stage in the context of trends (e.g., cooler temperatures promote less thaw while warmer temperatures promote more thaw), further adjustments of the CPTs, especially for snow depth, vegetation height/density, insulation, and soil moisture, are needed for the magnitudes of the probabilities to reflect reality.

For the diagnosis experiments, key results showed that, overall, the system responds as expected. When changes to thaw depth are low, active layer ice content is high while soil temperature is low (Fig. 6). Conversely, when changes to thaw depth are high, active layer ice content is low while soil temperature is high (Fig. 7). In both cases, the soil moisture node responds in an opposite manner in the diagnosis results as compared to the prognosis results, where lower soil moisture contributes to lower thaw depths in the former and higher thaw depths in the latter under the extreme low scenario; higher soil moisture contributes to higher thaw depths in the former and lower thaw depths in the latter under the extreme high scenario.

In both extreme scenarios, air temperature is predicted to be medium. Higher probabilities for the low and high air temperature scenarios were expected for the low and high thaw depth scenarios, respectively. Given the air temperature CPT, however, the results are unsurprising. Further experimentation revealed that the air temperature node appears to respond better when it is set to a uniform distribution (Beall, 2021). This indicates that CPTs in the middle nodes of the model may need further refinement. Additional testing revealed that soil temperature and snow depth seem to be driving many of the responses in the model. Improving these distributions may improve the model response as a whole.

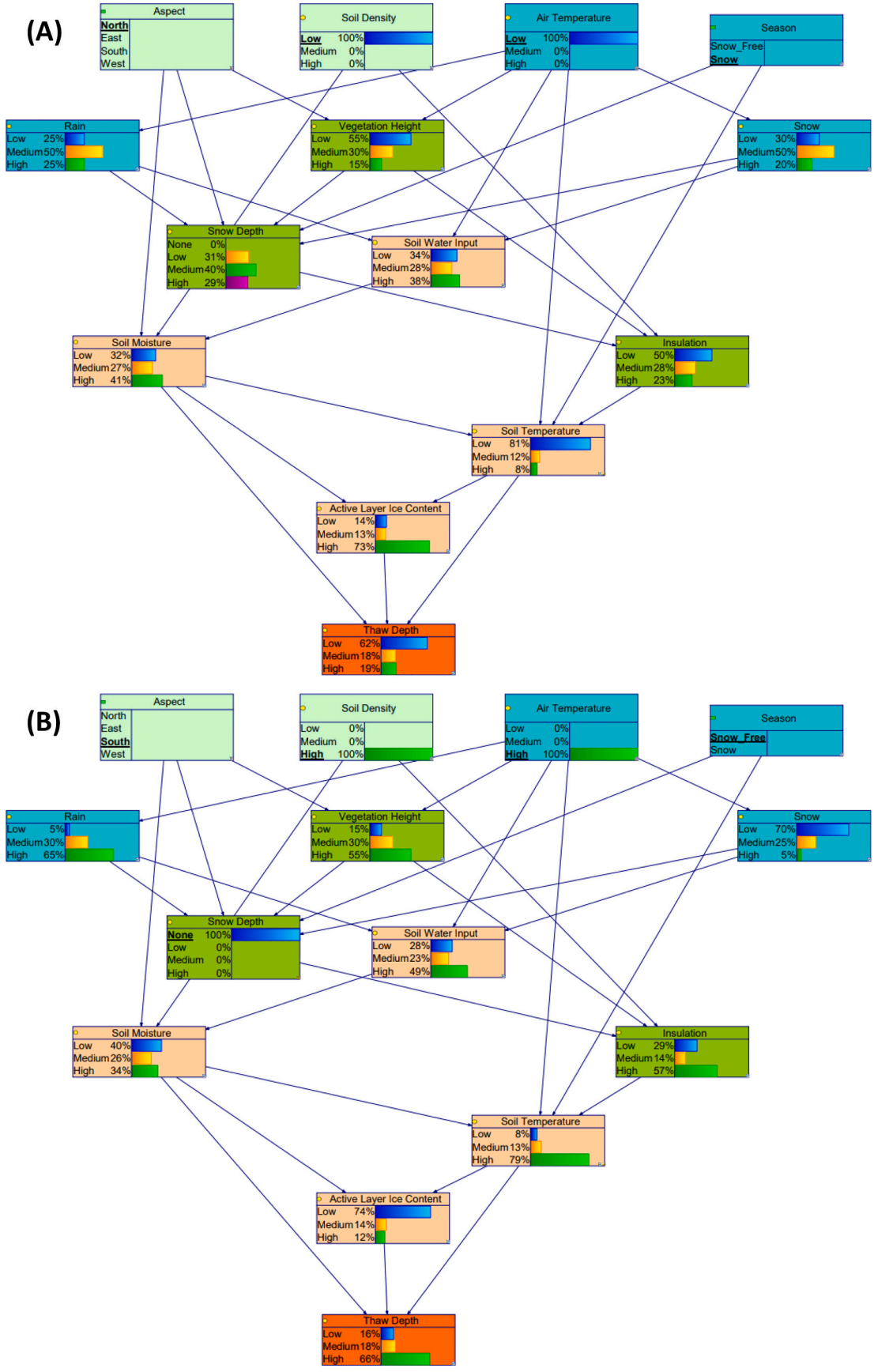

Fig. 5. Prognosis experiments where all nodes are informed using the (A) extreme low (i.e., north aspect, low soil density, low air temperature, and snow season) and (B) extreme high (i.e., south aspect, high soil density, high air temperature, and snow free season) scenarios.

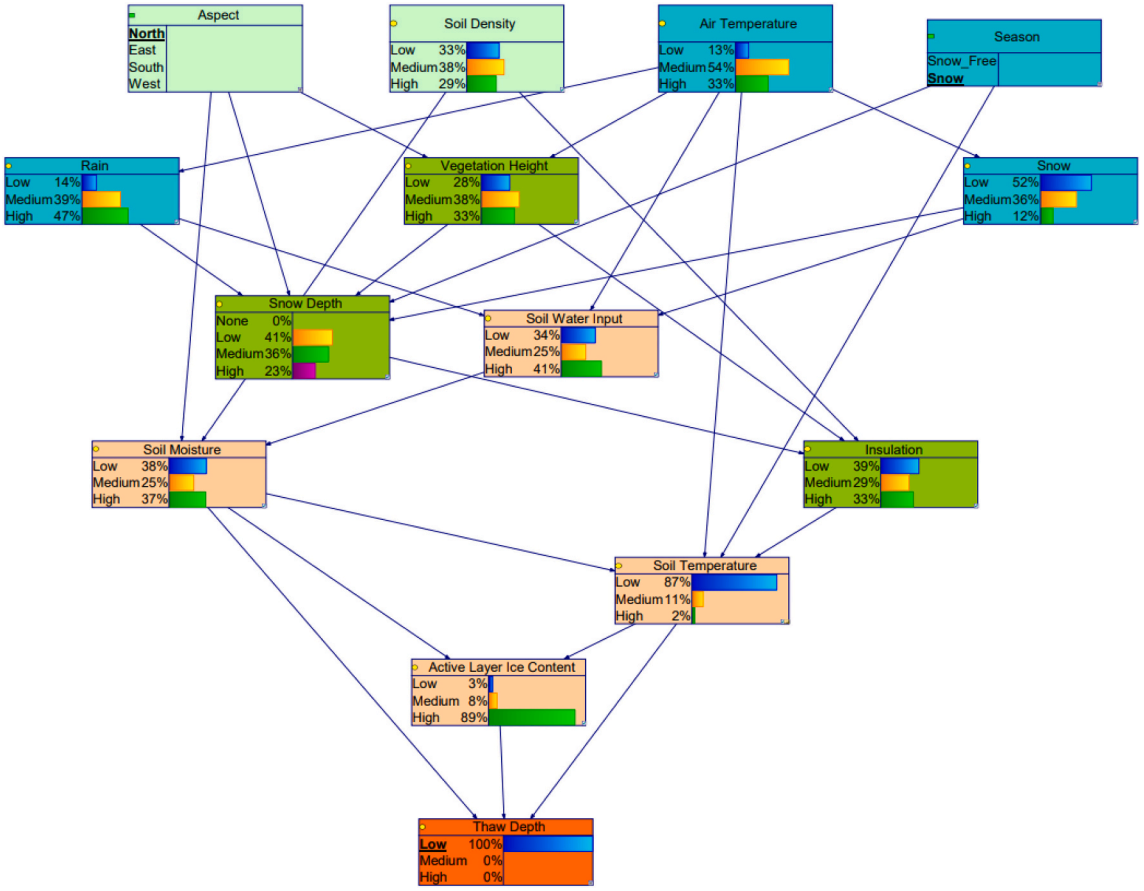

Fig. 6. Diagnosis experiment testing the extreme low scenario where the response of the system (i.e., thaw depth) is low, aspect is north, and season is snow.

3.5. Evaluation – case study with physical observations methods

Integrating observations from a local case study was the final step in the PermaBN development process. The criteria for determining which local case study to use were: (1) high spatiotemporal density of thaw depth observations, and (2) availability of additional variables at the same spatial and temporal scales. One site that meets these criteria is the Siksik Creek Basin in Trail Valley Creek, Northwest Territories, Canada where Wilcox et al. (2019) collected 1528 aspect, vegetation height, and frost table depth (i.e., thaw depth) measurements over the time period 2015-06-11 to 2015-08-20 across 10 transects.

The general Trail Valley Creek area is described in detail by Wilcox et al. (2019) and Grunberg et al. (2020). In summary, it is located approximately 45 km north of Inuvik and characterized by an 8-month-long snow cover period. The mean annual air temperature is about −7.9 °C to −10 °C, and mean annual precipitation is ~266 mm, of which ~66% falls as snow. Vegetation ranges from 0.5 to 3m in height, with the primary vegetation classes being "tundra" (e.g., *Sphagnum* moss), "birch" (e.g., *Betula glandulosa*), "alder" (e.g., *Alnus alnobetula*), and "channel" (e.g., *Salix* L.), as determined by Wilcox et al. (2019). The total thickness of ice-rich permafrost in the region is between 350 and 500 m, with the ALT varying between 0.5 and 0.8 m (Burn and Kokelj, 2009).

Wilcox et al. (2019) took environmental measurements along 10 transects and grids. These transects are several hundred meters apart and observation dates for each sampling campaign range by 2–3 days. The probability distribution of thaw depth from each transect was compared to see which transects could be grouped together for use in PermaBN. Only two transects (ss1 and ss1lys) had similar frost table depth (i.e., thaw depth) probability distributions for the entire June – August 2015 time period; these two transects also had their thaw depth measurements collected on the same days (Julian days 168, 173, 190, 194, 208, 222, and 232). A total of 146 observations were made along transect ss1, whereas 216 observations were made along transect ss1lys. It should be noted that aspect and vegetation height remained constant at this time scale; in other words, frost table depth is the only value to change throughout the study period. It should also be noted that the observations only represent the snow-free season in PermaBN, as observations were all made during the summer season. Therefore, physical observations that would be used to refine the snow season probabilities are not available.

The datasets for aspect and vegetation height were binned for direct use with the model as evidence for the vegetation height node. In the case of aspect, which is a decision node, observations were simply categorized as north, east, south, or west based on their degree value, where 0° – 45° and 315° – 360° is north, 45° – 135° is east, 135° – 225° is south, and 225° – 315° is west. As for vegetation height, since only three of the four vegetation classes were present in the ss1 and ss1lys transects, "tundra" (5–25 cm in height) was considered low, "alder" (80–150 cm) was considered medium, and "channel" (150–200 cm) was considered high. Probabilities for the vegetation height node were determined by counting how many low, medium, and high vegetation height values coincided with north, east, south, or west aspects, and then dividing by the total number within each aspect state. For example, if 25 of the 29 vegetation observations that were made on eastern aspects were classified as "tundra" (i.e., low vegetation height), then the probability of there being low vegetation on an east aspect is 25/29, or 86%.

Since physical observations are not available for the frost table depth variable's parent nodes of soil moisture, soil temperature, and active layer ice content, the frost table depth measurements could not be used to directly inform the model. Instead, the measurements for both the ss1 and ss1lys transects were binned according to the average Trail Valley

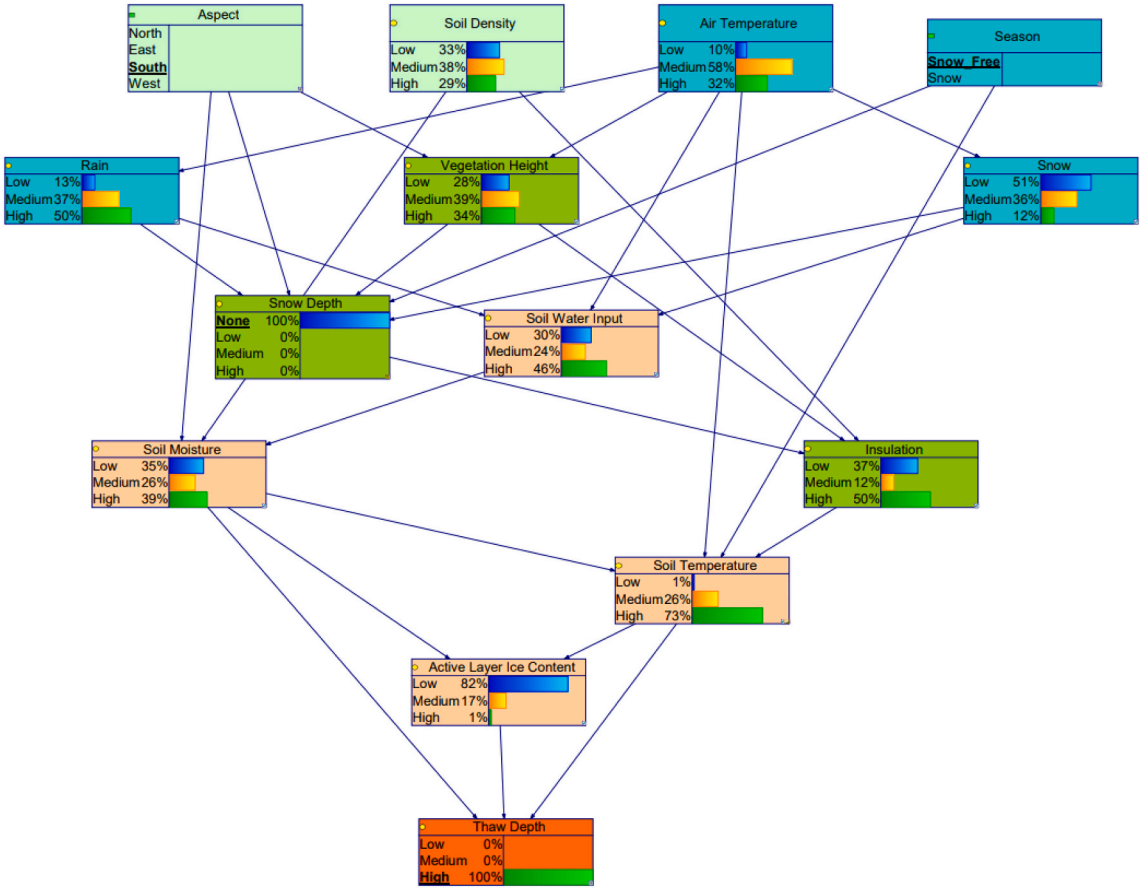

Fig. 7. Diagnosis experiment testing the extreme high scenario where the response of the system (i.e., thaw depth) is high, aspect is south, and season is snow free.

Creek ALT range of 50–80 cm cited in Wilcox et al. (2019), where low thaw depth was less than 50 cm, medium thaw depth was between 50 and 80 cm, and high thaw depth was greater than 80 cm; this yielded a distribution of 87% low, 13% medium, and 0% high thaw depths to be used as a benchmark for evaluating the performance of PermaBN. A set of 20 prognosis experiments (Appendix B) testing the effects of aspect/vegetation height, the extreme low and high scenarios, and the most likely Siksik Creek Basin aspect, soil density, air temperature, and soil temperature conditions were conducted to evaluate the ability of PermaBN to match the expected thaw depth distributions. A set of 15 diagnosis experiments (Appendix B) were also defined simply for exploratory purposes, as there is no way to conclusively evaluate the diagnosis performance given the limited parent node evidence available.

4. Results

Evaluation was conducted using the validated conceptual model in Fig. 4 and corresponding CPTs. The vegetation height node was informed with the probabilities determined from the physical observations. This resulted in a 100% probability of low vegetation on north and west aspects, 86%/10%/3% probability of low/medium/high vegetation on east aspects, and 83%/17%/0% probability of low/medium/high vegetation on south aspects, regardless of air temperature. Since observations are only available for the snow free season, the soil temperature CPT was modified to reflect that the snow and snow free seasons can have independent low, medium, and high probabilities, or in other words, that the boundaries for low, medium, and high soil temperature can differ depending on the season. The 20 prognosis experiments (Appendix B) were conducted to evaluate the ability of PermaBN to accurately predict the expected thaw depth distribution of 87% low thaw depth, 13% medium thaw depth, and 0% high thaw depth. The following paragraphs describe the key evaluation experiments.

Fig. 8 shows the thaw depth predictions for the snow free season for all aspects. For this season, PermaBN predicts a 48% chance of low thaw depth, 22% of medium thaw depth, and 29% thaw depth, for a margin of error of 39%, 5%, and 29%, respectively. Setting the aspect state only causes a slight shift in the thaw depth probabilities, with only a 1% increase in high thaw depth for north aspects, and 1% increase in low thaw depth for east and south aspects; west aspects retain the same overall distribution.

For the extreme low and high scenarios, a north aspect, low soil density, low air temperature, and snow free season results in a 60% chance of low thaw depth, 19% chance of medium thaw depth, and 21% chance of high thaw depth (Fig. 9A), for a margin of error of 27%, 2%, and 21%, respectively. A south aspect, high soil density, high air temperature, and snow free season results in a 54% chance of low thaw depth, 19% chance of medium thaw depth, and 27% high thaw depth (Fig. 9B), for a margin of error of 33%, 2%, and 27%, respectively.

Experiments also tested the most likely June – August conditions for the Siksik Creek Basin. A south aspect was selected based on the mean aspect for the ss1 and ss1lys transects, a low soil density based on site characterization by Grunberg et al. (2020) stating a ~ 5 cm soil organic layer and approximately equal mineral soil composition of clay, silt, and sand, and medium air temperature based on Grunberg et al. (2020)'s definition of summer as the time period with an average air temperature greater than or equal to 8 °C, their 1999–2018 mean annual cycle plot for summer air temperatures, and 2015 air temperature data from Inuvik station (Environment and Climate Change Canada, 2015). As seen in Fig. 10, this results in a 44% chance of low thaw depth, 24% chance of medium thaw depth, and 32% chance of high thaw depth, which is a margin of error of 43%, 7%, and 32%, respectively. However, when soil temperature is set to low in addition to the south aspect, low soil density,

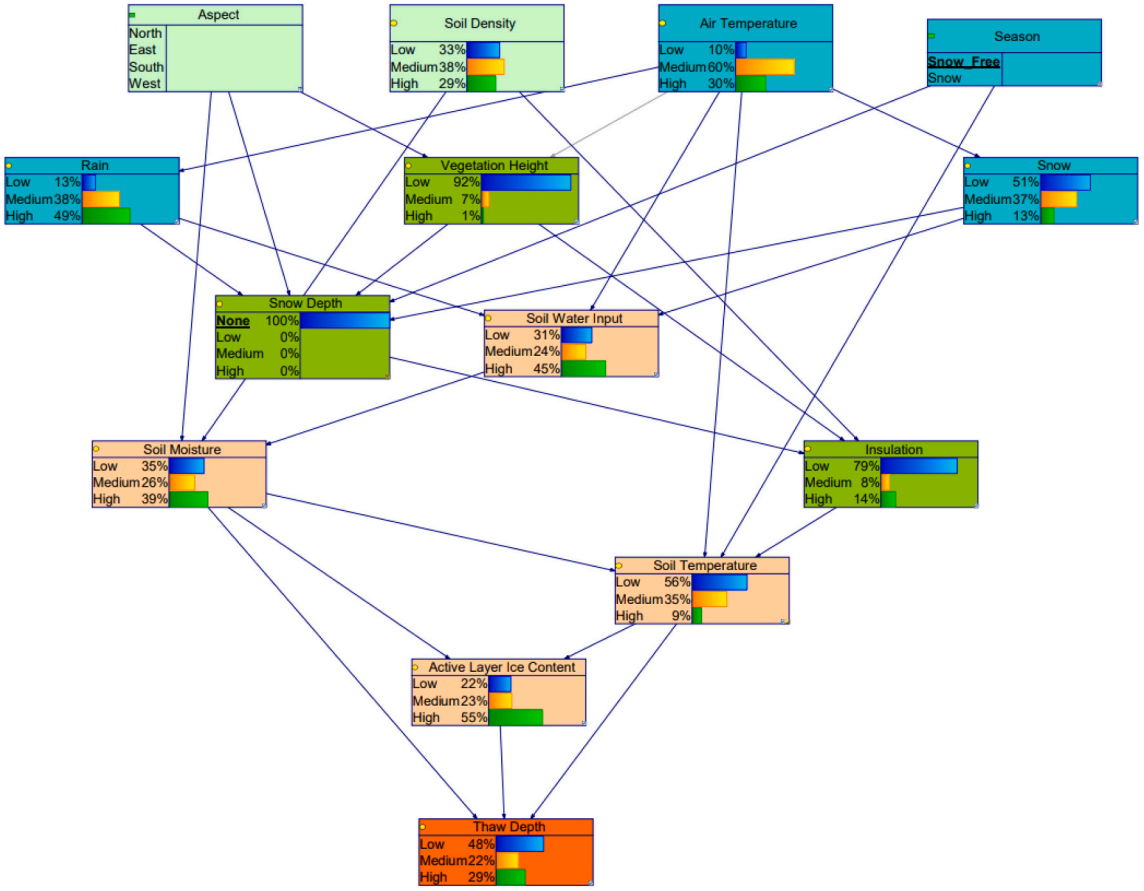

Fig. 8. PermaBN with informed vegetation height node prognosis predictions for snow free season.

and medium air temperature (Fig. 11), there is a 74% chance of low thaw depth, 16% chance of medium thaw depth, and 10% chance of high thaw depth, for a margin of error of 13%, 1%, and 10%, respectively. A final set of prognosis experiments testing the effects of a uniform soil temperature distribution were also conducted, with all tested aspect, soil density, and air temperature combinations yielding an approximately 34% chance of low thaw depth, 22% chance of medium thaw depth, and 44% chance of high thaw depth, for a margin of error of 53%, 5%, and 44%, respectively.

The 15 diagnosis experiments are primarily for exploratory purposes, as there is insufficient evidence within the parent nodes to properly evaluate the response of model. For all thaw depths in the snow free season, (low and high thaw depth experiments shown in Fig. 12A and B, respectively), there is strong favoring of medium air temperature, low insulation, fairly uniform soil moisture, low or medium soil temperature, and varying active layer ice content (high for low thaw depth, medium or high for medium thaw depth, and low or medium for high thaw depth). Similarly, experiments for low and high thaw depth for all aspects yielded medium air temperature, low insulation, uniform or high skewed soil moisture, low or high soil temperature (low or high thaw depth, respectively), and high or low active layer ice content (low or high thaw depth, respectively).

Remaining experiments continued to favor medium air temperatures, low insulation, and low or high active layer ice content depending on thaw depth; depending on the soil temperature scenario, soil moisture was either slightly low skewed (high soil temperature) or high skewed (low soil temperature). Finally, experiments testing likely aspect (south) and thaw depth (low or medium) conditions (Fig. 13) showed favoring of medium air temperature, fairy uniform soil density and soil moisture, low insulation, low or medium soil temperature (low or medium thaw depth, respectively), and high or medium active layer ice content (low or medium thaw depth, respectively). It is interesting to note that the south aspect and low thaw depth scenario yields a 12% chance of low air temperature, 54% chance of medium air temperature, and 33% chance of high air temperature, which is very close to the expected 17%, 53%, and 30% chance of low, medium, and high air temperatures for 2015-06-15 (Julian day 168) to 2015-08-20 (Julian day 232) at Inuvik station.

5. Discussion

5.1. Case study

The results of the Siksik Creek Basin case study demonstrate the ability of PermaBN to integrate multiple types of evidence into a single model. With that said, limited availability of physical observations proved to be a significant challenge, which limited our capacity to fully validate and evaluate the model. In particular, missing parent nodes make it difficult to quantitatively define the children CPTs in a robust manner. For example, the thaw depth node could not be determined through quantitative binning like the vegetation height node. It was also not possible to evaluate the snow season predictions since the data only spanned the June – August 2015 snow free period. More broadly, the manual adjustment of expertly assessed CPTs that were made on the basis of field observations from the Siksik Creek Basin mean that the solutions are not unique, providing further uncertainty in the node distributions as well as the specific cases within the CPT (e.g., the probability that thaw depth is low given low soil moisture, active layer ice content, and soil temperature). Another caveat to consider with this case study is that PermaBN was initially designed with the pan-Arctic and multiyear time scales in mind, such that the case study may not accurately reflect that initial design. For example, the air temperature

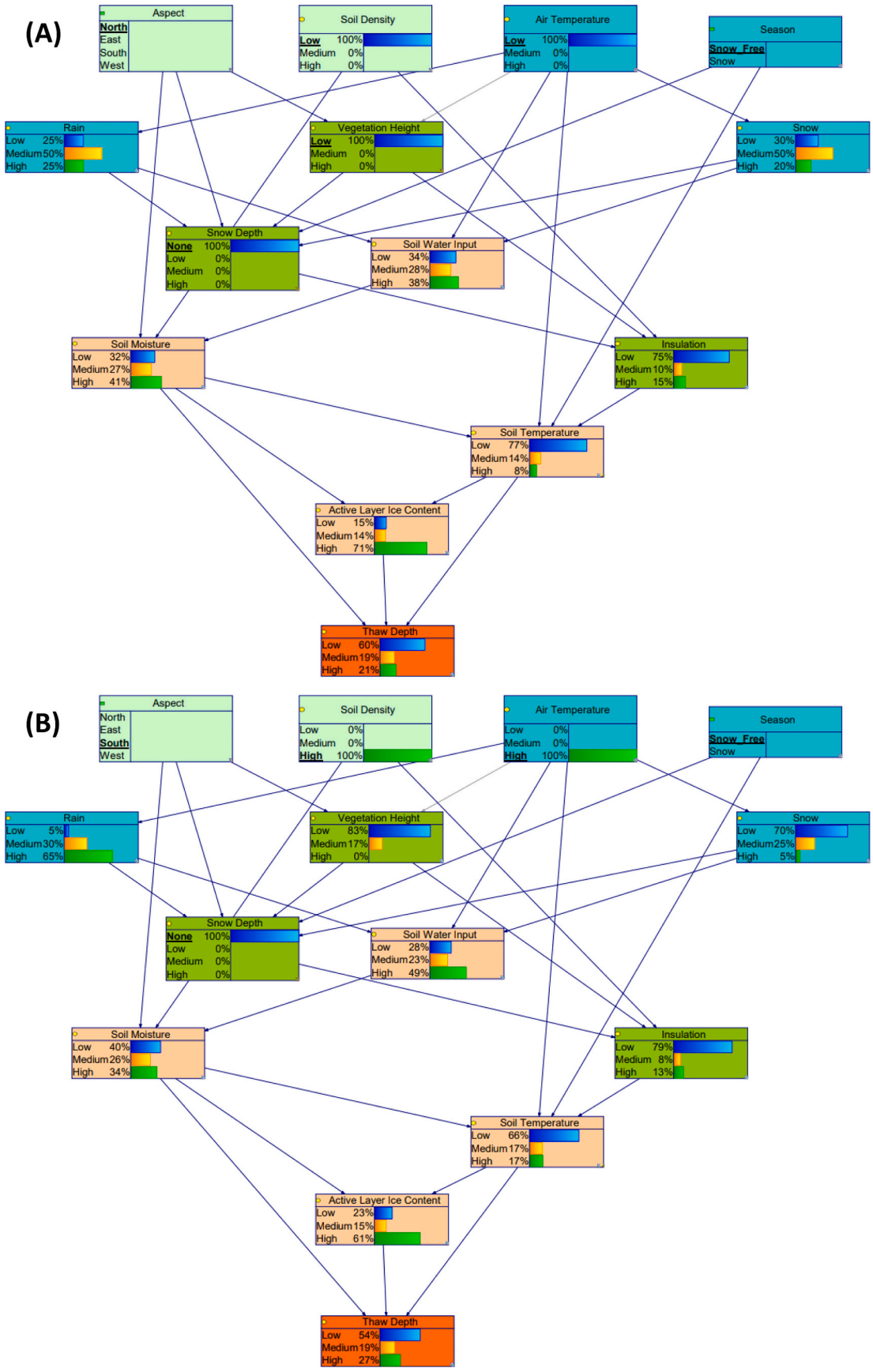

Fig. 9. PermaBN with informed vegetation height node prognosis predictions for (A) north aspect, low soil density, low air temperature, and snow free season and (B) south aspect, high soil density, high air temperature, and snow free season.

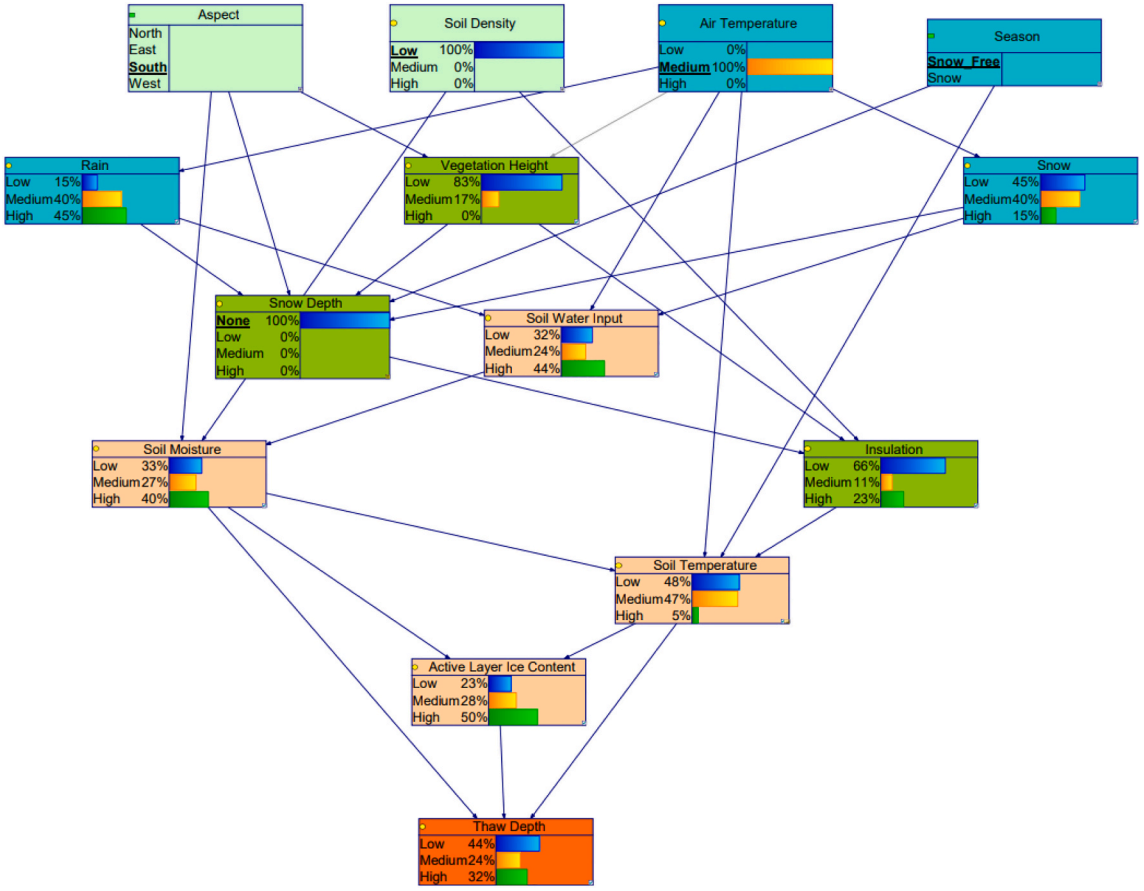

Fig. 10. PermaBN with informed vegetation height node prognosis predictions for south aspect, low soil density, medium air temperature, and snow free season.

joint distribution was initially defined with the assumption of decadal-scale warming temperatures in the Arctic, hence the higher probabilities for medium and high air temperatures as compared to low air temperatures. Without physical observations to determine the probability table, however, it is uncertain how accurate or inaccurate this assumption is for the Siksik Creek Basin for the June – August 2015 time period.

Nonetheless, the results of the most likely conditions prognosis and diagnosis experiments (i.e., those setting aspect as south, soil density as low, air temperature as medium, and/or soil temperature as low) suggest that PermaBN could perform relatively well when system conditions are known and that, in the case of the Siksik Creek Basin, applicable regional datasets (e.g., air temperatures for Inuvik) can be used to provide more informed expert assessment in the model. For instance, combining estimated boundaries of less than 8 °C for low air temperature, 8–15 °C for medium air temperature, and greater than 15 °C for high air temperature based on the work of Grunberg et al. (2020) with weather station data from Inuvik provided an estimated 17% chance of low air temperature, 53% chance of medium air temperature, and 30% chance of high air temperature. These estimations are quite similar to the original expert assessment values of a 10% chance for low, 60% chance of medium, and 30% chance of high air temperatures, as well as the diagnosis experiment with a south aspect, snow free season, and low thaw depth that yielded a 12% chance of low, 54% chance of medium, and 33% chance of high air temperatures. Overall, with refinement of the thaw depth parent nodes, it is likely that PermaBN could generate more accurate predictions. However, it was unexpected that the thaw depths strongly favored less thaw. Even when applying the thaw depth boundaries of less than 50 cm, 50–80 cm, and greater than 80 cm to all transects in the Siksik Creek Basin dataset, only 3% of depth measurements were expected to be high (i.e., greater than 80 cm), and 78% of measurements were expected to be low (i.e., less than 50 cm). This may indicate that permafrost in the Siksik Creek Basin has experienced less thaw than elsewhere in the broader Trail Valley Creek area or that the boundaries based on ALT for Trail Valley Creek are not as representative of the Siksik Creek Basin.

A final observation about the model evaluation stage is that aspect was not found to impact thaw depth by more than 1–2% between the different states. This may be due to the fact that aspect's primary contribution was to the vegetation height node and subsequently vegetation height's contribution to insulation. Since vegetation height for all aspects had an 83–100% chance of being low, and soil density had a fairly uniform distribution, insulation was always predominately low. The limited variability in insulation contributed to less influence on the soil temperature node, which is a key driver of thaw depth in the model. Likewise, the limited variability in the fairly uniform soil moisture node resulted in less influence on the soil temperature and thaw depths.

5.2. *Insights from PermaBN*

PermaBN is a unique proof-of-concept of a modeling approach that combines topography, meteorological conditions, soil characteristics, and vegetation into a single model. As seen in Table 1, there is no one model that accounts for all of the variables present in PermaBN. While the statistical model by Wilcox et al. (2019) accounts for vegetation and aspect, it does not include air temperature, precipitation, and soil parameters. Likewise, the statistical model by Hjort et al. (2018) accounts for certain soil parameters and slope, but excludes vegetation, air temperature, and precipitation, and the one by Aalto et al. (2018) accounts for air temperature, precipitation, soil organic carbon, and potential incoming solar radiation, but not vegetation or additional soil characteristics. Older, predominantly non-statistical models thoroughly

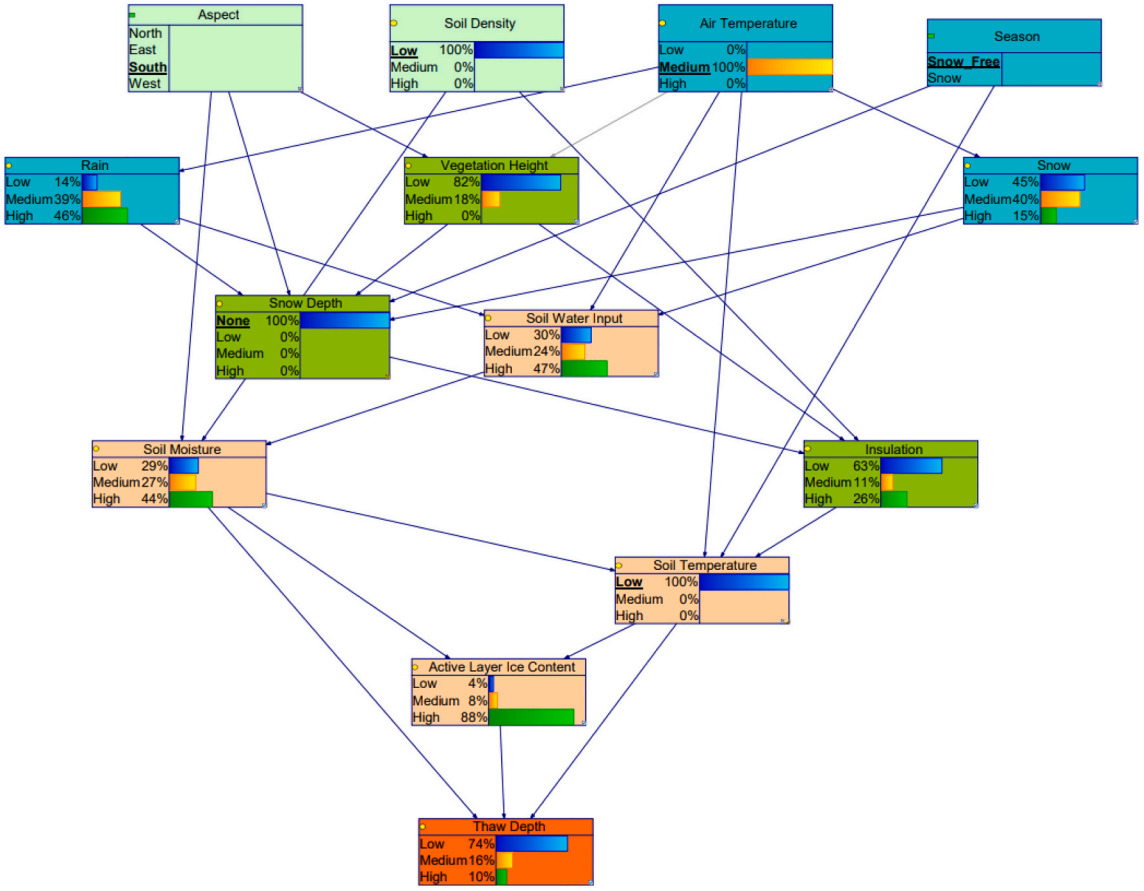

Fig. 11. PermaBN with informed vegetation height node prognosis predictions for south aspect, low soil density, medium air temperature, low soil temperature, and snow free season.

account for soil characteristics or thermal dynamics related to snow depth and moisture conditions but largely lack the inclusion of vegetation or atmospheric components other than air temperature. The closest model match appears to be the NEST model (Zhang et al. (2006), which includes vegetation, air temperature, precipitation, solar radiation, ground ice content, mineral vs. organic soil, and other soil thermal properties (i.e., thermal conductivity and geothermal heat flux), though it omits the explicit representation of soil moisture and soil temperature. Future testing of PermaBN could be done by comparing the results of the two models.

5.3. Limitations

As outlined in Chen and Pollino (2012), uncertainties in BNs can originate from incomplete understanding of the process(es) being modeled, incomplete data, or subjective biases in the expert assessments. BNs allow for explicit representation of uncertainty, but they cannot differentiate between different types of uncertainty, such as uncertainties with input data and model structure (Korb and Nicholson, 2004). While expert assessment datasets can help reduce uncertainties in model structure in particular, they are prone to introducing bias and epistemic uncertainty and may yield results that are accurate but not necessarily precise (Kuhnert et al., 2010; Webster and McLaughlin, 2014). Following proper methods and procedures when eliciting expert assessment datasets may help significantly reduce these uncertainties. Further, if this process is thought of as a sampling process, there will be better convergence to the 'truth' as more opinions are collected from experts per the central limit theorem. Exploring alternative quantitative methods for determining the CPTs could also help reduce uncertainties in the model. For instance, sensitivity analysis can allow for identification of missing or unneeded linkages, and act as an alternative evaluation method for determining which variables in the model are most influential; conditional probabilities can also be learned from algorithms, such as the Lauritzen – Spiegelhalter algorithm or Gibbs sampling (Chen and Pollino, 2012). Finally, the inclusion of decision nodes can limit the tools and algorithms available for use in the GeNIe software program. The inclusion of decision nodes results in the BN being classified as an "influence diagram," and some tools, such as the "sensitivity analysis" tool, are unavailable for use with influence diagrams within the software. The decision nodes would either need to be removed or converted to chance nodes prior to running these tools in GeNIe.

5.4. Future work

As development of BNs is often seen as an on-going process (Fox et al., 2017; McLaughlin and Packalen, 2021; Webster and McLaughlin, 2014), there are many avenues of future work that can be undertaken with PermaBN. Foremost could be addressing the limitations previously discussed by: (1) aiming to reduce uncertainty in the expertly assessed CPTs through more robust elicitation procedures, (2) conducting sensitivity analysis, (3) exploring algorithms for determining the CPTs, and (4) improving validation by finding or creating new datasets for evaluation. Related to the point on exploring algorithms for determining CPTs is calibration of the BN. Three types of calibration could be considered: (1) manual calibration, (2) optimization, and (3) probabilistic calibration. Manual calibration would entail manually manipulating the CPTs until the parent node yields the expected thaw depth response. Optimization would entail having an algorithm solve for the most likely scenario among the parent nodes given a particular state of the thaw

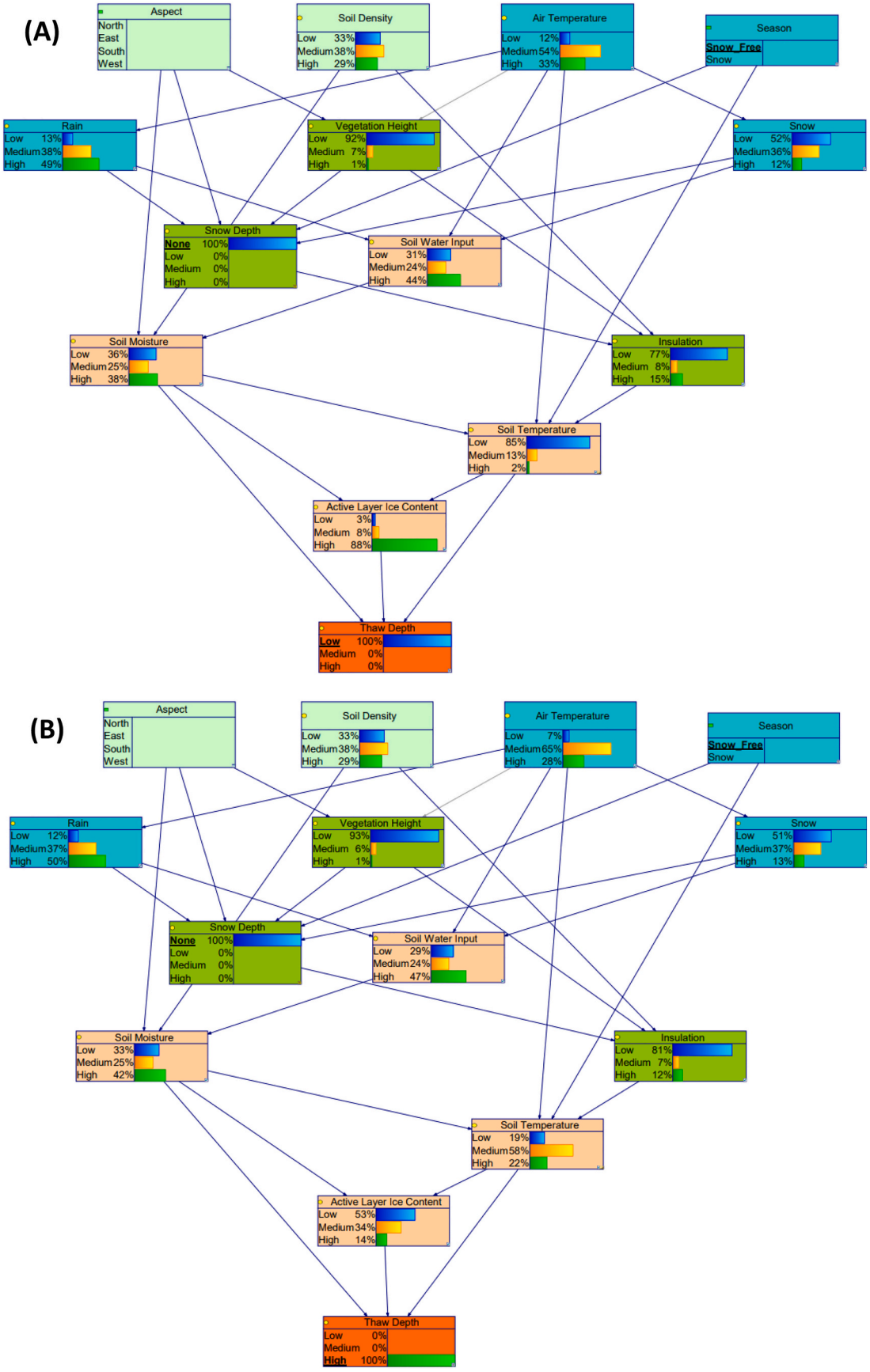

Fig. 12. PermaBN with informed vegetation height node diagnosis analysis for (A) low thaw depth and (B) high thaw depth for the snow free season.

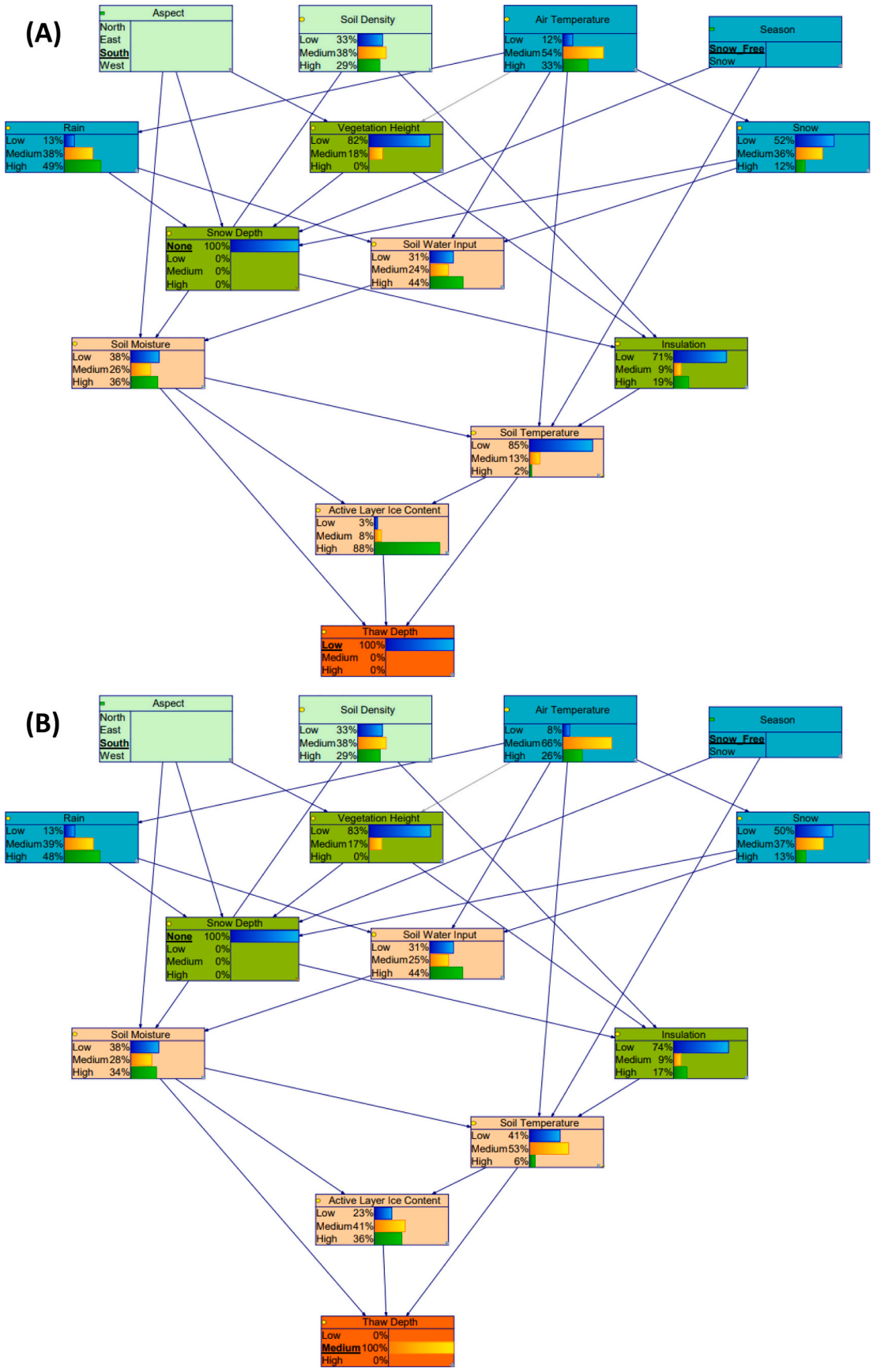

Fig. 13. PermaBN with informed vegetation height node diagnosis analysis for (A) south aspect and low thaw depth and (B) south aspect and medium thaw depth for the snow free season.

depth node; optimization would yield a single, unique result. In contrast, probabilistic calibration would explore many different scenarios for the parent nodes and report which of the scenarios are most likely. These methods of calibration are unique to BNs and would allow for the BN to perform better the next time it is run. Since manual calibration is time consuming and does not yield unique results, the recommended next step would be conducting optimization.

6. Conclusions

PermaBN is a Bayesian Network designed to assess permafrost thaw in the continuous permafrost region of the Arctic. It provides an innovative method for assessing permafrost thaw that allows for the integration of multiple types of evidence (e.g., physical observations, model outputs, and expert assessments) into a single model. This study outlined and discussed best BN model practices while providing a proof-of-concept of this unique modeling method. The framework presented offers a transparent modeling approach that is able to represent systems in data sparse regions such as the Arctic. Further, it facilitates the quantification of uncertainty through the use of probabilities.

The case study that was selected to further evaluate PermaBN also shed light on important aspects of both the model development and field data collection. For instance, physical observations allowed for reduction in uncertainty for those nodes that have data available; here, aspect and vegetation height data allowed for uncertainty in vegetation height conditions to be reduced since it was known which aspects contributed to which vegetation classes. Conversely, the model highlighted data gaps, such as long-term thaw depth measurements with concurrent meteorological and soil measurements. Filling these data gaps would certainly help validating models and furthering their development.

Aside from the benefits this modeling approach provides in data sparse regions, BNs also have the ability to engage a wider audience than traditional modeling approaches. Users without highly technical modeling skills can build BNs, and the graphical structure can easily be understood by and communicated to non-technical stakeholders. This is valuable in the context of interdisciplinary and participatory endeavors.

With future development of PermaBN to include a more robust validation procedure, additional variables, and/or integration with a risk assessment framework, PermaBN could be applied to carbon modeling studies, infrastructure hazard assessments, and policy decisions aimed at mitigation of and adaptation to permafrost thaw.

Declaration of Competing Interest

The authors declare that they have no known competing financial interests or personal relationships that could have appeared to influence the work reported in this paper.

Contributors

The expert assessments in Sections 3 and 4 were provided by Drs. Julie Loisel, David Cairns, and Oliver Frauenfeld of the Texas A&M University Department of Geography and Dr. Zenon Medina-Cetina of the Texas A&M University Zachry Department of Civil and Environmental Engineering. The pre-validation conceptual model borrows ideas from the Texas A&M University Arctic X-Grant team, and Evan Wilcox of Wilfrid Laurier University provided additional insight into the association of landscape variables with active layer thickness.

Funding sources

Graduate study (KB) was supported by a fellowship and an assistantship from Texas A&M University. Research was funded by a Texas A&M University X-Grant (JL) and NSF grant 1802838 (JL).

Appendix. Supplementary data

Supplementary data to this article can be found online at https://doi.org/10.1016/j.ecoinf.2022.101601.

References

Aalto, J., le Roux, P.C., Luoto, M., 2013. Vegetation mediates soil temperature and moisture in Arctic-alpine environments. Arct. Antarct. Alp. Res. 45 (4), 429–439. https://doi.org/10.1657/1938-4246-45.4.429.

Aalto, J., Karjalainen, O., Hjort, J., Luoto, M., 2018. Statistical forecasting of current and future Circum-Arctic ground temperatures and active layer thickness. Geophys. Res. Lett. 45 (10), 4889–4898. https://doi.org/10.1029/2018gl078007.

Abu-Hamdeh, N.H., Reeder, R.C., 2000. Soil thermal conductivity: effects of density, moisture, salt concentration, and organic matter. Soil Sci. Soc. Am. J. 64 (4), 1285–1290. https://doi.org/10.2136/sssaj2000.6441285x.

Aguilera, P.A., Fernandez, A., Fernandez, R., Rumi, R., Salmeron, A., 2011. Bayesian networks in environmental modelling. Environ. Model. Softw. 26 (12), 1376–1388. https://doi.org/10.1016/j.envsoft.2011.06.004.

Al-Yami, A.S.S., Schubert, J., Medina-Cetina, Z., Yu, O.-Y., 2010. Drilling expert system for the optimal design and execution of successful cementing practices. In: IADC/SPE Asia Pacific Drilling Technology Conference and Exhibition. SPE-135183-MS.

Anisimov, O.A., Shiklomanov, N.I., Nelson, F.E., 1997. Global warming and active-layer thickness: results from transient general circulation models. Glob. Planet. Chang. 15 (3–4), 61–77. https://doi.org/10.1016/s0921-8181(97)00009-x.

Arya, L.M., Paris, J.F., 1981. A Physicoempirical model to predict the soil-moisture characteristic from particle-size distribution and bulk-density data. Soil Sci. Soc. Am. J. 45 (6), 1023–1030. https://doi.org/10.2136/sssaj1981.03615995004500060004x.

BayesFusion, 2019. GeNIe, 2.4 ed.

Beall, K., 2021. Using a Bayesian Network Framework to Predict Permafrost Thaw in the Arctic. Master of Science. Texas A&M University.

Bintanja, R., Andry, O., 2017. Towards a rain-dominated Arctic. Nat. Clim. Chang. 7 (4), 263. https://doi.org/10.1038/nclimate3240.

Biskaborn, B.K., Lanckman, J.P., Lantuit, H., Elger, K., Streletskiy, D.A., Cable, W.L., Romanovsky, V.E., 2015. The new database of the global terrestrial network for permafrost (GTN-P). Earth Syst. Sci. Data 7 (2), 245–259. https://doi.org/10.5194/essd-7-245-2015.

Biskaborn, B.K., Smith, S.L., Noetzli, J., Matthes, H., Vieira, G., Streletskiy, D.A., Schoeneich, P., Romanovsky, V.E., Lewkowicz, A.G., Abramov, A., Allard, M., Boike, J., Cable, W.L., Christiansen, H.H., Delaloye, R., Diekmann, B., Drozdov, D., Etzelmuller, B., Grosse, G., Guglielmin, M., Ingeman-Nielsen, T., Isaksen, K., Ishikawa, M., Johansson, M., Johannsson, H., Joo, A., Kaverin, D., Kholodov, A., Konstantinov, P., Kroger, T., Lambiel, C., Lanckman, J.P., Luo, D.L., Malkova, G., Meiklejohn, I., Moskalenko, N., Oliva, M., Phillips, M., Ramos, M., Sannel, A.B.K., Sergeev, D., Seybold, C., Skryabin, P., Vasiliev, A., Wu, Q.B., Yoshikawa, K., Zheleznyak, M., Lantuit, H., 2019. Permafrost is warming at a global scale. Nat. Commun. 10, 11. https://doi.org/10.1038/s41467-018-08240-4.

Blok, D., Heijmans, M.M.P.D., Schaepman-Strub, G., Kononov, A.V., Maximov, T.C., Berendse, F., 2010. Shrub expansion may reduce summer permafrost thaw in Siberian tundra. Glob. Chang. Biol. 16 (4), 1296–1305. https://doi.org/10.1111/j.1365-2486.2009.02110.x.

Boike, J., Roth, K., Ippisch, O., 2003. Seasonal snow cover on frozen ground: Energy balance calculations of a permafrost site near Ny-Alesund, Spitsbergen. J. Geophys. Res.-Atmos. 108 (D1), 11. https://doi.org/10.1029/2001jd000939.

Burn, C.R., Kokelj, S.V., 2009. The environment and permafrost of the Mackenzie Delta area. Permafr. Periglac. Process. 20 (2), 83–105. https://doi.org/10.1002/ppp.655.

Chen, S.H., Pollino, C.A., 2012. Good practice in Bayesian network modelling. Environ. Model. Softw. 37, 134–145. https://doi.org/10.1016/j.envsoft.2012.03.012.

Comiso, J.C., Parkinson, C.L., Gersten, R., Stock, L., 2008. Accelerated decline in the Arctic Sea ice cover. Geophys. Res. Lett. 35 (1), 6. https://doi.org/10.1029/2007gl031972.

Das, R., Varela, P., Medina-Cetina, Z., 2019. The effect of Bayesian updating in the hazard assessment of submarine landslides. In: Offshore Technology Conference. D031S040R005.

Debolskiy, M.V., Nicolsky, D.J., Hock, R., Romanovsky, V.E., 2020. Modeling present and future permafrost distribution at the Seward Peninsula, Alaska. J. Geophys. Res. Earth Surf. 125 (8), 24. https://doi.org/10.1029/2019jf005355.

Douglas, T.A., Turetsky, M.R., Koven, C.D., 2020. Increased rainfall stimulates permafrost thaw across a variety of interior Alaskan boreal ecosystems. Npj Clim. Atmos. Sci. 3 (1), 7. https://doi.org/10.1038/s41612-020-0130-4.

Environment and Climate Change Canada, 2015. Historical Data - Inuvik A Station.

Evans, B.M., Walker, D.A., Benson, C.S., Nordstrand, E.A., Petersen, G.W., 1989. Spatial interrelationships between terrain, snow distribution and vegetation patterns at an arctic foothills site in Alaska. Holarct. Ecol. 12 (3), 270–278.

Fisher, J.P., Estop-Aragones, C., Thierry, A., Charman, D.J., Wolfe, S.A., Hartley, I.P., Murton, J.B., Williams, M., Phoenix, G.K., 2016. The influence of vegetation and soil characteristics on active-layer thickness of permafrost soils in boreal forest. Glob. Chang. Biol. 22 (9), 3127–3140. https://doi.org/10.1111/gcb.13248.

Flynn, M., Ford, J.D., Labbe, J., Schrott, L., Tagalik, S., 2019. Evaluating the effectiveness of hazard mapping as climate change adaptation for community planning in degrading permafrost terrain. Sustain. Sci. 14 (4), 1041–1056. https://doi.org/10.1007/s11625-018-0614-x.

Fox, W.E., Medina-Cetina, Z., Angerer, J., Varela, P.Y., Ryang Chung, J., 2017. Water quality & natural resource management on military training lands in Central Texas: improved decision support via Bayesian networks. Sustain. Water Qual. Ecol. 9-10, 39–52. https://doi.org/10.1016/j.swaqe.2017.03.001.

Frauenfeld, O.W., Zhang, T.J., Barry, R.G., Gilichinsky, D., 2004. Interdecadal changes in seasonal freeze and thaw depths in Russia. J. Geophys. Res. Atmos. 109 (D5), 12. https://doi.org/10.1029/2003jd004245.

Getoor, L., Rhee, J.T., Koller, D., Small, P., 2004. Understanding tuberculosis epidemiology using structured statistical models. Artif. Intell. Med. 30 (3), 233–256. https://doi.org/10.1016/j.artmed.2003.11.003.

Gockede, M., Kwon, M.J., Kittler, F., Heimann, M., Zimov, N., Zimov, S., 2019. Negative feedback processes following drainage slow down permafrost degradation. Glob. Chang. Biol. 25 (10), 3254–3266. https://doi.org/10.1111/gcb.14744.

Goodrich, L.E., 1978. Efficient numerical technique for one-dimensional thermal problems with phase-change. Int. J. Heat Mass Transf. 21 (5), 615–621. https://doi.org/10.1016/0017-9310(78)90058-3.

Goodrich, L.E., 1982. The influence of snow cover on the ground thermal regime. Can. Geotech. J. 19 (4), 421–432. https://doi.org/10.1139/t82-047.

Gruber, S., 2012. Derivation and analysis of a high-resolution estimate of global permafrost zonation. Cryosphere 6 (1), 221–233. https://doi.org/10.5194/tc-6-221-2012.

Grunberg, I., Wilcox, E.J., Zwieback, S., Marsh, P., Boike, J., 2020. Linking tundra vegetation, snow, soil temperature, and permafrost. Biogeosciences 17 (16), 4261–4279. https://doi.org/10.5194/bg-17-4261-2020.

Hanna, E., Cappelen, J., Fettweis, X., Mernild, S.H., Mote, T.L., Mottram, R., Steffen, K., Ballinger, T.J., Hall, R., 2020. Greenland surface air temperature changes from 1981 to 2019 and implications for ice-sheet melt and mass-balance change. Int. J. Climatol. 17. https://doi.org/10.1002/joc.6771.

Hjort, J., Karjalainen, O., Aalto, J., Westermann, S., Romanovsky, V.E., Nelson, F.E., Etzelmuller, B., Luoto, M., 2018. Degrading permafrost puts Arctic infrastructure at risk by mid-century. Nat. Commun. 9, 9. https://doi.org/10.1038/s41467-018-07557-4.

Holland, P.G., Steyn, D.G., 1975. Vegetational responses to latitudinal variations in slope angle and aspect. J. Biogr. 2 (3), 179–183. https://doi.org/10.2307/3037989.

Hugelius, G., Loisel, J., Chadburn, S., Jackson, R.B., Jones, M., MacDonald, G., Marushchak, M., Olefeldt, D., Packalen, M., Siewert, M.B., Treat, C., Turetsky, M., Voigt, C., Yu, Z.C., 2020. Large stocks of peatland carbon and nitrogen are vulnerable to permafrost thaw. Proc. Natl. Acad. Sci. U. S. A. 117 (34), 20438–20446. https://doi.org/10.1073/pnas.1916387117.

IPCC, 2013. Climate Change 2013: The Physical Science Basis. Contribution of Working Group I to the Fifth Assessment Report of the Intergovernmental Panel on Climate Change. Cambridge University Press, Cambridge, United Kingdom and New York, NY, USA.

Jafarov, E.E., Marchenko, S.S., Romanovsky, V.E., 2012. Numerical modeling of permafrost dynamics in Alaska using a high spatial resolution dataset. Cryosphere 6 (3), 613–624. https://doi.org/10.5194/tc-6-613-2012.

Jan, A., Painter, S.L., 2020. Permafrost thermal conditions are sensitive to shifts in snow timing. Environ. Res. Lett. 15 (8), 12. https://doi.org/10.1088/1748-9326/ab8ec4.

Jorgenson, M.T., Osterkamp, T.E., 2005. Response of boreal ecosystems to varying modes of permafrost degradation. Can. J. For. Res. 35 (9), 2100–2111. https://doi.org/10.1139/x05-153.

Jorgenson, M.T., Romanovsky, V., Harden, J., Shur, Y., O'Donnell, J., Schuur, E.A.G., Kanevskiy, M., Marchenko, S., 2010. Resilience and vulnerability of permafrost to climate change. Can. J. For. Res. 40 (7), 1219–1236. https://doi.org/10.1139/x10-060.

Jorgenson, M.T., Kanevskiy, M., Shur, Y., Moskalenko, N., Brown, D.R.N., Wickland, K., Striegl, R., Koch, J., 2015. Role of ground ice dynamics and ecological feedbacks in recent ice wedge degradation and stabilization. J. Geophys. Res. Earth Surf. 120 (11), 2280–2297. https://doi.org/10.1002/2015jf003602.

Kaikkonen, L., Parviainen, T., Rahikainen, M., Uusitalo, L., Lehikoinen, A., 2021. Bayesian networks in environmental risk assessment: a review. Integr. Environ. Assess. Manag. 17 (1), 62–78. https://doi.org/10.1002/ieam.4332.

Karjalainen, O., Aalto, J., Luoto, M., Westermann, S., Romanovsky, V.E., Nelson, F.E., Etzelmuller, B., Hjort, J., 2019. Circumpolar permafrost maps and geohazard indices for near-future infrastructure risk assessments. Scientific Data 6, 16. https://doi.org/10.1038/sdata.2019.37.

Keller, F., 1992. Automated mapping of mountain permafrost using the program permakart within the geographical information-system arc info. In: Permafrost and Periglacial Processes, Vol 3, No 2, Apr-Jun 1992: Permafrost and Periglacial Environments in Mountain Areas, pp. 133–138.

Kjaerulff, U., 1995. DHUGIN – a computational system for dynamic time-sliced Bayesian networks. Int. J. Forecast. 11 (1), 89–111. https://doi.org/10.1016/0169-2070(94)02003-8.

Kokelj, S.V., Jorgenson, M.T., 2013. Advances in thermokarst research. Permafr. Periglac. Process. 24 (2), 108–119. https://doi.org/10.1002/ppp.1779.

Korb, K.B., Nicholson, A.E., 2004. Bayesian Artificial Intelligence. Chapman & Hall/CRC, London, UK.

Koven, C.D., Riley, W.J., Stern, A., 2013. Analysis of permafrost thermal dynamics and response to climate change in the CMIP5 earth system models. J. Clim. 26 (6), 1877–1900. https://doi.org/10.1175/jcli-d-12-00228.1.

Kudryavtsev, V.A., Garagulya, L.S., Kondrat'yeva, K.A., Melamed, V.G., 1974. Fundamentals of Frost Forecasting in Geological Engineering Investigations. Hanover, NH, Cold Regions Research and Engineering Laboratory.

Kuhnert, P.M., Martin, T.G., Griffiths, S.P., 2010. A guide to eliciting and using expert knowledge in Bayesian ecological models. Ecol. Lett. 13 (7), 900–914. https://doi.org/10.1111/j.1461-0248.2010.01477.x.

Kwok, R., Cunningham, G.F., Wensnahan, M., Rigor, I., Zwally, H.J., Yi, D., 2009. Thinning and volume loss of the Arctic Ocean sea ice cover: 2003-2008. J. Geophys. Res. Oceans 114, 16. https://doi.org/10.1029/2009jc005312.

Laidre, K.L., Stirling, I., Lowry, L.F., Wiig, O., Heide-Jorgensen, M.P., Ferguson, S.H., 2008. Quantifying the sensitivity of arctic marine mammals to climate-induced habitat change. Ecol. Appl. 18 (2), S97–S125. https://doi.org/10.1890/06-0546.1.

Lawrence, D.M., Swenson, S.C., 2011. Permafrost response to increasing Arctic shrub abundance depends on the relative influence of shrubs on local soil cooling versus large-scale climate warming. Environ. Res. Lett. 6 (4), 8. https://doi.org/10.1088/1748-9326/6/4/045504.

Lawrence, D.M., Slater, A.G., Romanovsky, V.E., Nicolsky, D.J., 2008. Sensitivity of a model projection of near-surface permafrost degradation to soil column depth and representation of soil organic matter. J. Geophys. Res. Earth Surf. 113 (F2), 14. https://doi.org/10.1029/2007jf000883.

Lee, H., Swenson, S.C., Slater, A.G., Lawrence, D.M., 2014. Effects of excess ground ice on projections of permafrost in a warming climate. Environ. Res. Lett. 9 (12), 8. https://doi.org/10.1088/1748-9326/9/12/124006.

Liljedahl, A.K., Boike, J., Daanen, R.P., Fedorov, A.N., Frost, G.V., Grosse, G., Hinzman, L.D., Iijma, Y., Jorgenson, J.C., Matveyeva, N., Necsoiu, M., Raynolds, M. K., Romanovsky, V.E., Schulla, J., Tape, K.D., Walker, D.A., Wilson, C.J., Yabuki, H., Zona, D., 2016. Pan-Arctic ice-wedge degradation in warming permafrost and its influence on tundra hydrology. Nat. Geosci. 9 (4), 312. https://doi.org/10.1038/ngeo2674.

Loranty, M.M., Abbott, B.W., Blok, D., Douglas, T.A., Epstein, H.E., Forbes, B.C., Jones, B. M., Kholodov, A.L., Kropp, H., Malhotra, A., Mamet, S.D., Myers-Smith, I.H., Natali, S.M., O'Donnell, J.A., Phoenix, G.K., Rocha, A.V., Sonnentag, O., Tape, K.D., Walker, D.A., 2018. Reviews and syntheses: changing ecosystem influences on soil thermal regimes in northern high-latitude permafrost regions. Biogeosciences 15 (17), 5287–5313. https://doi.org/10.5194/bg-15-5287-2018.

Lunardini, V.J., 1978. Theory of N-Factors and Correlation of Data. Proceedings of the Third International Conference on Permafrost. National Research Council of Canada Ottawa, Edmonton, Alberta, Canada.

Lunardini, V.J., 1981. Heat Transfer in Cold Climates. Van Nostrand Reinhold Co.

Marcot, B.G., Steventon, J.D., Sutherland, G.D., McCann, R.K., 2006. Guidelines for developing and updating Bayesian belief networks applied to ecological modeling and conservation. Can. J. For. Res. 36 (12), 3063–3074. https://doi.org/10.1139/x06-135.

McLaughlin, J.W., Packalen, M.S., 2021. Peat carbon vulnerability to projected climate warming in the Hudson Bay lowlands, Canada: a decision support tool for land use planning in peatland dominated landscapes. Front. Earth Sci. 9 (608) https://doi.org/10.3389/feart.2021.650662.

Medina-Cetina, Z., Nadim, F., 2008. Stochastic design of an early warning system. Georisk 2 (4), 223–236. https://doi.org/10.1080/17499510802086777.
-Assessment and Management of Risk for Engineered Systems and Geohazards.

Meentemeyer, V., Zippin, J., 1981. Soil-moisture and texture controls of selected parameters of needle ice growth. Earth Surf. Process. Landf. 6 (2), 113–125. https://doi.org/10.1002/esp.3290060205.

Meredith, M., Sommerkorn, M., Cassotta, S., Derksen, C., Ekaykin, A., Hollowed, A., Kofinas, G., Mackintosh, A., Melbourne-Thomas, J., Muelbert, M.M.C., Ottersen, G., Pritchard, H., Schuur, E.A.G., 2019. IPCC special report on the ocean and cryosphere in a changing climate. In: Pörtner, H.-O., Roberts, D.C., Masson-Delmotte, V., Zhai, P., Tignor, M., Poloczanska, E., Mintenbeck, K., Alegría, A., Nicolai, M., Okem, A., Petzold, J., Rama, B., Weyer, N.M. (Eds.), Polar Regions.

Myers-Smith, I.H., Forbes, B.C., Wilmking, M., Hallinger, M., Lantz, T., Blok, D., Tape, K. D., Macias-Fauria, M., Sass-Klaassen, U., Levesque, E., Boudreau, S., Ropars, P., Hermanutz, L., Trant, A., Collier, L.S., Weijers, S., Rozema, J., Rayback, S.A., Schmidt, N.M., Schaepman-Strub, G., Wipf, S., Rixen, C., Menard, C.B., Venn, S., Goetz, S., Andreu-Hayles, L., Elmendorf, S., Ravolainen, V., Welker, J., Grogan, P., Epstein, H.E., Hik, D.S., 2011. Shrub expansion in tundra ecosystems: dynamics, impacts and research priorities. Environ. Res. Lett. 6 (4), 15. https://doi.org/10.1088/1748-9326/6/4/045509.

Myers-Smith, I.H., Kerby, J.T., Phoenix, G.K., Bjerke, J.W., Epstein, H.E., Assmann, J.J., John, C., Andreu-Hayles, L., Angers-Blondin, S., Beck, P.S.A., Berner, L.T., Bhatt, U. S., Bjorkman, A.D., Blok, D., Bryn, A., Christiansen, C.T., Cornelissen, J.H.C., Cunliffe, A.M., Elmendorf, S.C., Forbes, B.C., Goetz, S.J., Hollister, R.D., de Jong, R., Loranty, M.M., Macias-Fauria, M., Maseyk, K., Normand, S., Olofsson, J., Parker, T. C., Parmentier, F.J.W., Post, E., Schaepman-Strub, G., Stordal, F., Sullivan, P.F., Thomas, H.J.D., Tommervik, H., Treharne, R., Tweedie, C.E., Walker, D.A., Wilmking, M., Wipf, S., 2020. Complexity revealed in the greening of the Arctic. Nat. Clim. Chang. 10 (2), 106–117. https://doi.org/10.1038/s41558-019-0688-1.

Nelson, F.E., 1986. Permafrost distribution in Central Canada – applications of a climate-based predictive model. Ann. Assoc. Am. Geogr. 76 (4), 550–569. https://doi.org/10.1111/j.1467-8306.1986.tb00136.x.

Nelson, F.E., Outcalt, S.I., 1987. A computational method for prediction and regionalization of permafrost. Arct. Alp. Res. 19 (3), 279–288. https://doi.org/10.2307/1551363.

Nicolsky, D.J., Romanovsky, V.E., 2018. Modeling long-term permafrost degradation. J. Geophys. Res. Earth Surf. 123 (8), 1756–1771. https://doi.org/10.1029/2018jf004655.

Oelke, C., Zhang, T.J., 2004. A model study of circum-arctic soil temperatures. Permafr. Periglac. Process. 15 (2), 103–121. https://doi.org/10.1002/ppp.485.

Olefeldt, D., Goswami, S., Grosse, G., Hayes, D., Hugelius, G., Kuhry, P., McGuire, A.D., Romanovsky, V.E., Sannel, A.B.K., Schuur, E.A.G., Turetsky, M.R., 2016. Circumpolar distribution and carbon storage of thermokarst landscapes. Nat. Commun. 7, 11. https://doi.org/10.1038/ncomms13043.

O'Neill, H.B., Burn, C.R., 2012. Physical and temporal factors controlling the development of near-surface ground ice at Illisarvik, western Arctic coast, Canada. Can. J. Earth Sci. 49 (9), 1096–1110. https://doi.org/10.1139/e2012-043.
Park, H., Sherstiukov, A.B., Fedorov, A.N., Polyakov, I.V., Walsh, J.E., 2014. An observation-based assessment of the influences of air temperature and snow depth on soil temperature in Russia. Environ. Res. Lett. 9 (6), 7. https://doi.org/10.1088/1748-9326/9/6/064026.
Pastick, N.J., Jorgenson, M.T., Wylie, B.K., Nield, S.J., Johnson, K.D., Finley, A.O., 2015. Distribution of near-surface permafrost in Alaska: estimates of present and future conditions. Remote Sens. Environ. 168, 301–315. https://doi.org/10.1016/j.rse.2015.07.019.
Pearl, J., 2009. Causality: Models, Reasoning, and Inference, 2nd ed. Cambridge University Press, United States of America.
Petzold, D.E., Mulhern, T., 1987. Vegetation distributions along lichen-dominated slopes of opposing aspect in the Eastern Canadian Sub-Arctic. Arctic 40 (3), 221–224.
Pistone, K., Eisenman, I., Ramanathan, V., 2014. Observational determination of albedo decrease caused by vanishing Arctic Sea ice. Proc. Natl. Acad. Sci. U. S. A. 111 (9), 3322–3326. https://doi.org/10.1073/pnas.1318201111.
Qin, Y., Chen, J.S., Yang, D.W., Wang, T.H., 2018. Estimating seasonally frozen ground depth from historical climate data and site measurements using a Bayesian model. Water Resour. Res. 54 (7), 4361–4375. https://doi.org/10.1029/2017wr022185.
Riseborough, D., 2007. The effect of transient conditions on an equilibrium permafrost-climate model. Permafr. Periglac. Process. 18 (1), 21–32. https://doi.org/10.1002/ppp.579.
Riseborough, D., Shiklomanov, N., Etzelmuller, B., Gruber, S., Marchenko, S., 2008. Recent advances in permafrost modelling. Permafr. Periglac. Process. 19 (2), 137–156. https://doi.org/10.1002/ppp.615.
Rouse, W.R., Douglas, M.S.V., Hecky, R.E., Hershey, A.E., Kling, G.W., Lesack, L., Marsh, P., McDonald, M., Nicholson, B.J., Roulet, N.T., Smol, J.P., 1997. Effects of climate change on the freshwaters of arctic and subarctic North America. Hydrol. Process. 11 (8), 873–902. https://doi.org/10.1002/(sici)1099-1085(19970630)11:8<873::aid-hyp510>3.0.co;2-6.
Schuur, E.A.G., Mack, M.C., 2018. Ecological response to permafrost thaw and consequences for local and global ecosystem services. Annu. Rev. Ecol. Evol. Syst. 49 (49), 279–301. https://doi.org/10.1146/annurev-ecolsys-121415-032349.
Schuur, E.A.G., Vogel, J.G., Crummer, K.G., Lee, H., Sickman, J.O., Osterkamp, T.E., 2009. The effect of permafrost thaw on old carbon release and net carbon exchange from tundra. Nature 459 (7246), 556–559. https://doi.org/10.1038/nature08031.
Schuur, E.A.G., McGuire, A.D., Schadel, C., Grosse, G., Harden, J.W., Hayes, D.J., Hugelius, G., Koven, C.D., Kuhry, P., Lawrence, D.M., Natali, S.M., Olefeldt, D., Romanovsky, V.E., Schaefer, K., Turetsky, M.R., Treat, C.C., Vonk, J.E., 2015. Climate change and the permafrost carbon feedback. Nature 520 (7546), 171–179. https://doi.org/10.1038/nature14338.
Screen, J.A., Simmonds, I., 2010. The central role of diminishing sea ice in recent Arctic temperature amplification. Nature 464 (7293), 1334–1337. https://doi.org/10.1038/nature09051.
Screen, J.A., Simmonds, I., 2012. Declining summer snowfall in the Arctic: causes, impacts and feedbacks. Clim. Dyn. 38 (11−12), 2243–2256. https://doi.org/10.1007/s00382-011-1105-2.
Serreze, M.C., Barry, R.G., 2014. The Arctic Climate System, 2nd ed. Cambridge University Press, New York, NY.
Serreze, M.C., Meier, W.N., 2019. The Arctic's sea ice cover: trends, variability, predictability, and comparisons to the Antarctic. Ann. N. Y. Acad. Sci. 1436 (1), 36–53. https://doi.org/10.1111/nyas.13856.
Serreze, M.C., Holland, M.M., Stroeve, J., 2007. Perspectives on the Arctic's shrinking sea-ice cover. Science 315 (5818), 1533–1536. https://doi.org/10.1126/science.1139426.
Serreze, M.C., Barrett, A.P., Stroeve, J.C., Kindig, D.N., Holland, M.M., 2009. The emergence of surface-based Arctic amplification. Cryosphere 3 (1), 11–19. https://doi.org/10.5194/tc-3-11-2009.
Smith, M.W., Riseborough, D.W., 1996. Permafrost monitoring and detection of climate change. Permafr. Periglac. Process. 7 (4), 301–309. https://doi.org/10.1002/(sici)1099-1530(199610)7:4<301::aid-ppp231>3.0.co;2-r.
Stiegler, C., Johansson, M., Christensen, T.R., Mastepanov, M., Lindroth, A., 2016. Tundra permafrost thaw causes significant shifts in energy partitioning. Tellus Ser. B Chem. Phys. Meteorol. 68, 11. https://doi.org/10.3402/tellusb.v68.30467.
Stroeve, J.C., Markus, T., Boisvert, L., Miller, J., Barrett, A., 2014. Changes in Arctic melt season and implications for sea ice loss. Geophys. Res. Lett. 41 (4), 1216–1225. https://doi.org/10.1002/2013gl058951.
Tao, J., Reichle, R.H., Koster, R.D., Forman, B.A., Xue, Y., 2017. Evaluation and enhancement of permafrost modeling with the NASA catchment land surface model. J. Adv. Model. Earth Syst. 9 (7), 2771–2795. https://doi.org/10.1002/2017ms001019.
Turetsky, M.R., Abbott, B.W., Jones, M.C., Anthony, K.W., Olefeldt, D., Schuur, E.A.G., Grosse, G., Kuhry, P., Hugelius, G., Koven, C., Lawrence, D.M., Gibson, C., Sannel, A.B.K., McGuire, A.D., 2020. Carbon release through abrupt permafrost thaw. Nat. Geosci. 13 (2), 138. https://doi.org/10.1038/s41561-019-0526-0.
Uusitalo, L., 2007. Advantages and challenges of Bayesian networks in environmental modelling. Ecol. Model. 203 (3–4), 312–318. https://doi.org/10.1016/j.ecolmodel.2006.11.033.
Varela Gonzalez, P.Y., 2017. Probabilistic Risk Mapping Coupling Bayesian Networks and GIS, and Bayesian Model Calibration of Submarine Landslides. Doctor of Philosophy. Texas A&M University.
Wainwright, H.M., Liljedahl, A.K., Dafflon, B., Ulrich, C., Peterson, J.E., Gusmeroli, A., Hubbard, S.S., 2017. Mapping snow depth within a tundra ecosystem using multiscale observations and Bayesian methods. Cryosphere 11 (2), 857–875. https://doi.org/10.5194/tc-11-857-2017.
Wang, K., Jafarov, E., Overeem, I., 2020. Sensitivity evaluation of the Kudryavtsev permafrost model. Sci. Total Environ. 720, 13. https://doi.org/10.1016/j.scitotenv.2020.137538.
Weber, P., Medina-Oliva, G., Simon, C., Iung, B., 2012. Overview on Bayesian networks applications for dependability, risk analysis and maintenance areas. Eng. Appl. Artif. Intell. 25 (4), 671–682. https://doi.org/10.1016/j.engappai.2010.06.002.
Webster, K.L., McLaughlin, J.W., 2014. Application of a Bayesian belief network for assessing the vulnerability of permafrost to thaw and implications for greenhouse gas production and climate feedback. Environ. Sci. Pol. 38, 28–44. https://doi.org/10.1016/j.envsci.2013.10.008.
Westermann, S., Langer, M., Boike, J., Heikenfeld, M., Peter, M., Etzelmuller, B., Krinner, G., 2016. Simulating the thermal regime and thaw processes of ice-rich permafrost ground with the land-surface model CryoGrid 3. Geosci. Model Dev. 9 (2), 523–546. https://doi.org/10.5194/gmd-9-523-2016.
Wilcox, E.J., Keim, D., de Jong, T., Walker, B., Sonnentag, O., Sniderhan, A.E., Mann, P., Marsh, P., 2019. Tundra shrub expansion may amplify permafrost thaw by advancing snowmelt timing. Arctic Sci. 5 (4), 202–217. https://doi.org/10.1139/as-2018-0028.
Woodard, D.L., Shiklomanov, A.N., Kravitz, B., Hartin, C., Bond-Lamberty, B., 2021. A permafrost implementation in the simple carbon-climate model hector. Geosci. Model Dev. Discuss. 2021, 1–21. https://doi.org/10.5194/gmd-2020-377.
Young, K.L., Woo, M.K., Edlund, S.A., 1997. Influence of local topography, soils, and vegetation on microclimate and hydrology at a high Arctic site, Ellesmere Island, Canada. Arct. Alp. Res. 29 (3), 270–284. https://doi.org/10.2307/1552141.
Yu, O., Medina-Cetina, Z., Guikema, S.D., 2012. Integrated approach for the optimal selection of environmentally friendly drilling systems. Int. J. Energy Environ. Eng. 3 (25) https://doi.org/10.1186/2251-6832-3-25.
Zhang, T., Osterkamp, T.E., Stamnes, K., 1996. Influence of the depth hoar layer of the seasonal snow cover on the ground thermal regime. Water Resour. Res. 32 (7), 2075–2086. https://doi.org/10.1029/96wr00996.
Zhang, Y., Chen, W.J., Riseborough, D.W., 2006. Temporal and spatial changes of permafrost in Canada since the end of the Little Ice Age. J. Geophys. Res.-Atmos. 111 (D22), 14. https://doi.org/10.1029/2006jd007284.
Zhang, Y., Sherstiukov, A.B., Qian, B.D., Kokelj, S.V., Lantz, T.C., 2018. Impacts of snow on soil temperature observed across the circumpolar north. Environ. Res. Lett. 13 (4) https://doi.org/10.1088/1748-9326/aab1e7, 10.
Zheng, L., Overeem, I., Wang, K., Clow, G.D., 2019. Changing Arctic River dynamics cause localized permafrost thaw. J. Geophys. Res. Earth Surf. 124 (9), 2324–2344. https://doi.org/10.1029/2019jf005060.
Zwieback, S., Westermann, S., Langer, M., Boike, J., Marsh, P., Berg, A., 2019. Improving permafrost modeling by assimilating remotely sensed soil moisture. Water Resour. Res. 55 (3), 1814–1832. https://doi.org/10.1029/2018wr023247.